BASIC RESEARCH www.jasn.org

Indoleamine 2,3-dioxygenase-1, a Novel Therapeutic Target for Post-Vascular Injury Thrombosis in CKD

Joshua A. Walker,[1,2] Sean Richards,[1] Stephen A. Whelan,[3] Sung Bok Yoo,[1] Teresa L. Russell,[1] Nkiruka Arinze,[4] Saran Lotfollahzadeh,[1] Marc A. Napoleon,[1] Mostafa Belghasem,[5] Norman Lee,[3] Laura M. Dember,[6,7] Katya Ravid,[2,8] and Vipul C. Chitalia[1,10,9]

Due to the number of contributing authors, the affiliations are listed at the end of this article.

ABSTRACT

Background CKD, characterized by retained uremic solutes, is a strong and independent risk factor for thrombosis after vascular procedures. Uremic solutes such as indoxyl sulfate (IS) and kynurenine (Kyn) mediate prothrombotic effect through tissue factor (TF). IS and Kyn biogenesis depends on multiple enzymes, with therapeutic implications unexplored. We examined the role of indoleamine 2,3-dioxyge-nase-1 (IDO-1), a rate-limiting enzyme of kynurenine biogenesis, in CKD-associated thrombosis after vascu-lar injury.

Methods IDO-1 expression in mice and human vessels was examined. IDO-1$^{-/-}$ mice, IDO-1 inhibitors, an adenine-induced CKD, and carotid artery injury models were used.

Results Both global IDO-1$^{-/-}$ CKD mice and IDO-1 inhibitor in wild-type CKD mice showed reduced blood Kyn levels, TF expression in their arteries, and thrombogenicity compared with respective controls. Several advanced IDO-1 inhibitors downregulated TF expression in primary human aortic vascular smooth muscle cells specifically in response to uremic serum. Further mechanistic probing of arteries from an IS-specific mouse model, and CKD mice, showed upregulation of IDO-1 protein, which was due to inhibition of its polyubiquitination and degradation by IS in vascular smooth muscle cells. In two cohorts of patients with advanced CKD, blood IDO-1 activity was significantly higher in sera of study participants who subsequently developed thrombosis after endovascular interventions or vascular surgery.

Conclusion Leveraging genetic and pharmacologic manipulation in experimental models and data from human studies implicate IS as an inducer of IDO-1 and a perpetuator of the thrombotic milieu and supports IDO-1 as an antithrombotic target in CKD.

JASN 32: 2834–2850, 2021. doi: https://doi.org/10.1681/ASN.2020091310

Atherothrombotic cardiovascular disease (CVD) is highly prevalent in patients with CKD.[1–3] Among CVD manifestations, patients with CKD in particular are at a higher risk of unprovoked arterial thrombosis driving cardiovascular and cerebrovascular events. Numerous studies also demonstrate a significantly heightened risk of thrombosis after vascular interventions in patients with CKD.[4–13] The vascular intervention can be an endovascular procedure, such as angioplasty and stenting, or vascular surgery such as coronary or femoral-popliteal bypass or arteriovenous fistula (AVF) creation. Given the number of vascular procedures performed in coronaries, peripheral arteries, and hemodialysis vascular accesses in patients with CKD, thrombosis after these interventions becomes an important clinical problem. Yet, there is a dearth of mechanistic studies in this area.

Received September 14, 2020. Accepted August 16, 2021.

Published online ahead of print. Publication date available at www.jasn.org.

Correspondence: Dr. Vipul Chitalia, Boston University Medical Center, Evans Biomedical Research Center, X-530 Boston, MA 02118. Email: vichital@bu.edu

The CKD state is characterized by retention of several solutes, collectively referred to as uremic toxins, which are considered nontraditional CVD risk factors.[15] Emerging evidence indicates a causal link between uremic toxins and atherothrombotic disease in CKD mouse models and patients.[15–20] Of these solutes, tryptophan (Trp) metabolites, such as indoxyl sulfate (IS) and kynurenine (Kyn), are particularly vasculotoxic on the basis of previous work by our group and that of others.[17–19,21] IS and Kyn increased tissue factor (TF) protein expression in vessels mediated by aryl hydrocarbon receptor (AHR) signaling.[17,19,20,22] These studies defined the IS/Kyn–AHR–TF thrombosis axis in endothelial cells and vascular smooth muscle cells (vSMCs) in CKD mice driving thrombosis after vascular injury. This axis was subsequently validated in two independent clinical cohorts with participants across different CKD stages.[23]

Although the prothrombotic role of both IS and Kyn is emerging,[17,19,20,22] relationships between them in driving a hyperthrombotic uremic milieu remain elusive. Both Kyn and IS are derived from Trp. Trp is converted to indole by the intestinal microbiome, which further undergoes biotransformation in the liver to generate indolic solutes. Accordingly, dietary modification and alteration of the microbiome are being explored as potential approaches to reduce the concentrations of indolic solutes.[24] In contrast, Kyn biogenesis includes the indoleamine 2,3-dioxygenase (IDO) family of enzymes as a key regulator of its synthesis. The majority of dietary Trp is metabolized by the enzymes IDO-1 and Trp 2,3-dixoygenase (TDO).[25,26] Although both these enzymes mediate the oxidative cleavage of Trp to *N*-formylkynurenine, which is subsequently converted to Kyn, they exhibit distinct differences. TDO has a lower affinity for Trp compared with IDO-1[27] and is mainly expressed in the liver.[28] IDO-1 is an inducible enzyme, and its expression is limited to the immune cells (such as dendritic cells),[29] vSMC,[30] and endothelial cells.[31] Given IDO-1 expression in vessels and its central role in regulating Kyn production, we posited that inhibiting IDO-1 activity is likely to reduce thrombosis in the CKD milieu.

Significance Statement

Patients with CKD are at a markedly higher risk of thrombosis after vascular procedures. Uremic solutes, such as indoxyl sulfate and kynurenine, are important contributors to this complication through tissue factor (TF), a trigger of the extrinsic coagulation cascade. This study examines the role of indoleamine 2,3-dioxygenase-1 (IDO-1), a key enzyme in kynurenine biogenesis, in thrombotic complications in CKD. Using genomic and pharmacological approaches, this study demonstrates that IDO-1 is a critical regulator of TF and thrombosis after vascular injury in CKD mice. Indoxyl sulfate upregulates IDO-1, creating a feedback-forward loop. IDO-1 activity was higher in patients with CKD, who developed thrombosis after vascular interventions. This study identifies IDO-1 as a therapeutic target and uncovers crosstalk between uremic solutes, perpetuating their toxic effect.

METHODS

Animals

IDO-1$^{-/-}$ mice were purchased from the Jackson Laboratory (stock 005867). IDO-1$^{-/-}$ mouse line was generated using a targeting vector that replaced exons 3–5 of IDO-1 with a cassette containing β-galactosidase and neomycin resistance genes. This vector was electroporated into 129/SvJ–derived embryonic stem cells with correctly targeted clones injected into blastocysts. Chimeric male mice were bred with female C57BL/6 mice to produce heterozygous and offspring were backcrossed for more than ten generations to C57BL/6. Animals were maintained and bred on a C57BL/6 background under the supervision of the Boston University Animal Core Facility after the Institutional Animal Care and Use Committee protocol number AN-15449.2016.03. C57BL/6 (Jackson Laboratory) wild-type mice were used for other assays (Supplemental Materials and Methods and Supplemental References).

Induction of CKD in IDO$^{+/+}$ and IDO-1$^{-/-}$ Mice

Female 8–10-week-old IDO$^{+/+}$ and IDO- 1$^{-/-}$ mice were fed either a normal mouse diet or a diet supplemented with 0.25% adenine (Research Diets Inc., New Brunswick, NJ) for a total of 14 days to induce CKD, as previously described.[20]

Treatment of 1-Methyl Tryptophan and Thrombosis Assay and Analysis of Blood

To examine if inhibiting IDO-1 can decrease TF in a CKD model *in vivo*, C57/BL6J IDO$^{+/+}$ mice were pretreated with 1-MT (50 mg/kg, 2× daily, intraperitoneally) 2 days before inducing CKD with a 0.25% adenine–supplemented diet. The diet and 1-methyl tryptophan (1-MT) administration continued for a total of 4 days, with the carotid artery injury model of thrombosis performed on day 5. The carotid artery blood flow was measured by an ultrasound probe.[20] Time to occlusion (TtO) was determined when blood flow was <0.30 ml/min. The thrombosis assays are typically conducted in a carotid artery because it can be gently dissected without creating injury.[32,33] The dissection allows the placement of a $FeCL_3$ strip on the posterior wall of the artery and an ultrasound probe around the artery to measure blood flow.[34] These processes can only be conducted on carotid or femoral arteries given their location and ease of dissection, but not in the aorta located in the intrathoracic cavity. For other assays, such as western blots, the aorta was used due to higher protein yield from the explanted thoracic aorta. Plasma samples were analyzed for BUN and creatinine using the QuantiChrom Urea Assay Kit (DIUR-100) (BioAssay Systems, Hayward, CA) and a Creatinine Estimation Kit (Sigma MAK080) using the manufacturer's instructions.

Immunoprecipitation and Ubiquitination Assay

HEK293T or primary human aortic vSMCs were grown to 50%–60% confluence. Before harvest, the cells were treated with 10 μM MG132 to inhibit proteasomal degradation or DMSO as a control. The lysates underwent immunoprecipitation using anti-Flag or anti–IDO-1 antibody and protein A agarose beads (Santa Cruz Biotechnology, sc-2001). The blots were probed with ubiquitin antibody.

Dialysis Access Consortium Clopidogrel Prevention of Early AV Fistula Thrombosis and Thrombosis in Myocardial Infarction-II Patient Sera

Sera from two previous National Institutes of Health (NIH) clinical trials, the Dialysis Access Consortium Clopidogrel Prevention of Early AV Fistula Thrombosis (DAC-Fistula) trial[35] and the Thrombosis in Myocardial Infarction-II (TIMI-II) trial[36] were obtained from the National Institute of Diabetes and Digestive and Kidney Diseases Central Repository (DAC-Fistula), BioLINCC and the National Heart, Lung, and Blood Institute (NHLBI) Central Repository (TIMI-II) (IRB H-26367).

Statistical Analysis

Data were analyzed using a nonparametric Welch's *t* test or ANOVA with Tukey's multiple pairwise comparisons, as indicated. Significance was accepted as $P<0.05$.

Targeted metabolomics/mass spectrometry, immunoblotting, immunohistochemistry, and cells and reagents including antibodies and IDO-1 inhibitors (Supplemental Tables 1 and 2), and the carotid artery injury model of vascular thrombosis[19] are detailed in the Supplemental Methods.

RESULTS

IDO-1 Is Expressed in Endothelial Cells and vSMCs of Arteries in Rodents and Humans

We first confirmed the expression of IDO-1 in the arteries of mice and humans. Specificity of an IDO-1 antibody was confirmed using an isotype control antibody and using arteries from IDO-$1^{-/-}$ mice in immunohistochemistry (IHC) assay (Figure 1A). Although IDO-1 was expressed in endothelial cells (Figure 1a, black arrowhead) and in the smooth muscle cells in the medial layer of aorta (Figure 1A, orange arrowhead), its expression was more prominent in endothelial cells. IDO-1 expression was absent in the aorta of IDO-$1^{-/-}$ mice. The cellular expression of IDO-1 was confirmed with a double-label immunofluorescence (IF) assay (Figure 1, B and C) using CD31 and α-smooth muscle actin (α-SMA) as markers of endothelial cells and vSMCs, respectively. IDO-1 was detected in both cell types in mice aortas. Similarly, human temporal arteries were probed (Figure 1D) through staining of serial tissue sections with Pentachrome stain to identify muscle (red), nuclei (black), and connective tissue (blue). Black and yellow arrowheads point to endothelial and vSMCs in the intima and media, respectively. IDO-1 was expressed in endothelial cells and more prominently in vSMCs. These observations were further supported in a double-label IF assay using human temporal arteries (Figure 1, E and F). Collectively, these data confirmed the expression of IDO-1 in mouse and human arteries.

Global IDO-1 Knockout Mice Show Reduced TF Expression and Thrombogenicity

Having demonstrated IDO-1 expression in arteries, we next examined its role in thrombogenicity in the uremic milieu. Among different CKD models,[37] we used the adenine-induced CKD model (Supplemental Figure 1A). Adenine is converted to 2,8-dihydroxy adenine crystals in the renal interstitium, resulting in tubular atrophy and tubulointerstitial fibrosis (Supplemental Figure 1B).[38–40] Prolonged exposure to adenine (>12–16 weeks) is known to induce vascular calcification, bone mineral disease, and other related complications.[38,39] However, 2 weeks of 0.25% adenine in the diet was sufficient to increase BUN, IS, and Kyn levels in mice corresponding to levels in patients with advanced CKD.[20,23,41,42] This protocol served as a good model to examine post-vascular injury thrombosis in CKD without the confounding effect of other cardiovascular manifestations (*e.g.*, vascular calcification) observed with a protracted adenine diet. The 2-week adenine exposure specifically damaged kidneys, and did not alter heart and liver histology (Supplemental Figure 1C).

Thrombogenicity was examined in these mice using a $FeCL_3$-induced carotid artery injury, a model that is used extensively in arterial thrombosis studies.[43–46] Mice on an adenine diet had a 1.6-fold increase in TF expression in the aorta compared with control mice ($P=0.03$, Supplemental Figure 2, A and B) and significantly shortened TtO (Supplemental Figure 2C).

With further validation of the 2-week adenine diet model recapitulating the thrombotic uremic milieu,[20] next we examined the influence of IDO-1 on thrombogenicity in the uremic milieu. A group of 8–10-week-old female IDO-$1^{-/-}$ mice were fed a 0.25% adenine diet for 14 days, followed by the carotid artery injury model.[19,20] The baseline blood flow in all four groups ranged between 1.7 and 1.9 ml/min and showed no differences between $IDO^{-/-}$ and $IDO^{+/+}$ mice. $IDO^{+/+}$ mice and those on a normal diet served as controls (Figure 2A) ($n=7$ per group). BUN and creatinine were significantly elevated in mice on an adenine diet compared with those on a normal diet (Figure 2, B and C). No differences were observed in these parameters between $IDO^{+/+}$ and $IDO^{-/-}$ CKD mice.

Kyn levels increased six-fold in IDO-$1^{+/+}$ mice on adenine diet compared with mice on normal diet (normal diet

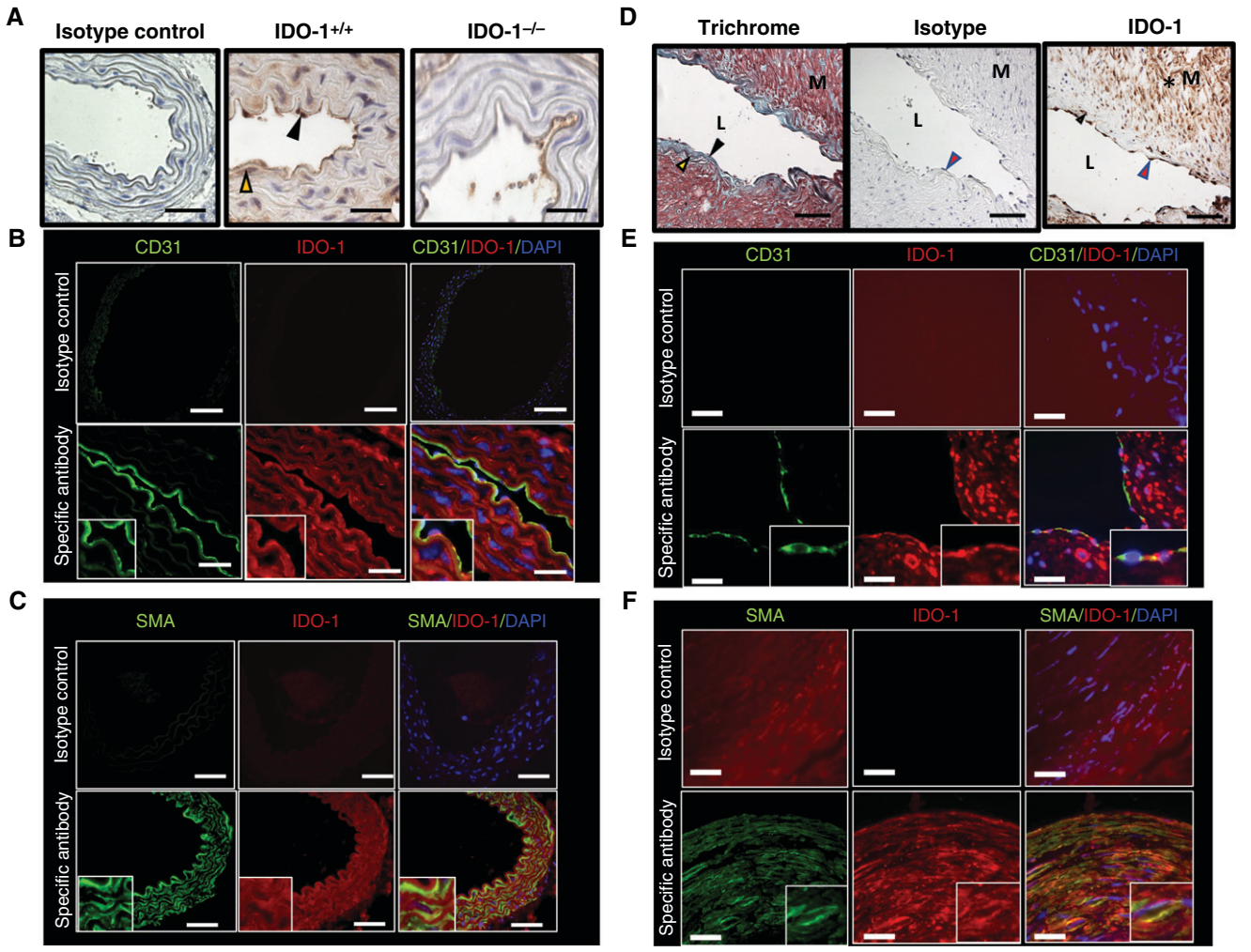

Figure 1. Expression of IDO-1 in arteries of normal mice and humans. (A) Thoracic aortas of 8-week-old C57BL/6 IDO-$1^{+/+}$ mice and IDO-$1^{-/-}$ mice were embedded and stained with an isotype control antibody or IDO-1 antibody and counterstained by hematoxylin. Images at 200× magnification from five different mice from each group are shown. Black and orange arrowheads point to the endothelial and vSMC in the intima and media, respectively. Scale bar = 100 μM. (B) Paraffin-embedded thoracic aortas of 8-week-old C57BL/6 mice were stained with IDO-1, and CD31 antibody. Isotype antibodies served as controls. DAPI-stained nuclei. Alexa fluor 488 and 594 antibodies were used as secondary antibodies. Representative images with 600× magnification from five different mice are shown. The inserts show a part of the aorta with CD31 and IDO-1. Scale bar = 100 μM. (C) Aortas were stained as above with SMA, IDO-1, and isotype antibodies, which served as controls. Representative images with 400× magnification from five different mice are shown. The inserts show a part of the aorta with SMA and IDO-1. Scale bar = 30 μM. (D) Serial sections of a temporal artery of a 46-year-old male stained with the modified Russell Movat Pentachrome stain (to delineate the elastic lamina), isotype control, or IDO-1 antibody and counterstained with hematoxylin are shown. Representative images from three independent human participants are shown at 100× magnification. Pentachrome-stain colors elastic fiber, collagen, muscles, proteoglycans, and reticular fibers. L = lumen, M = media. Black arrowhead points to the intima and yellow arrowhead points to internal elastic lamina. Red arrowheads point to the endothelial and the black asterisk depicts vSMCs in the media. Scale bar = 50 μM. (E) Sections of temporal arteries were stained with IDO-1 and CD31 antibody. Isotype antibodies served as controls. DAPI-stained nuclei. Alexa fluor 488 and 594 antibodies were used as secondary antibodies. Representative images with 600× magnification from three independent human participants are shown. The inserts show a part of the aorta with CD31 and IDO-1. Scale bar = 100 μM. (F) Sections of temporal arteries were stained as above with SMA and IDO-1 and isotype antibodies served as controls. Representative images with 400× magnification from five different mice are shown. The inserts show a part of the aorta with SMA and IDO-1. Scale bar = 30 μM.

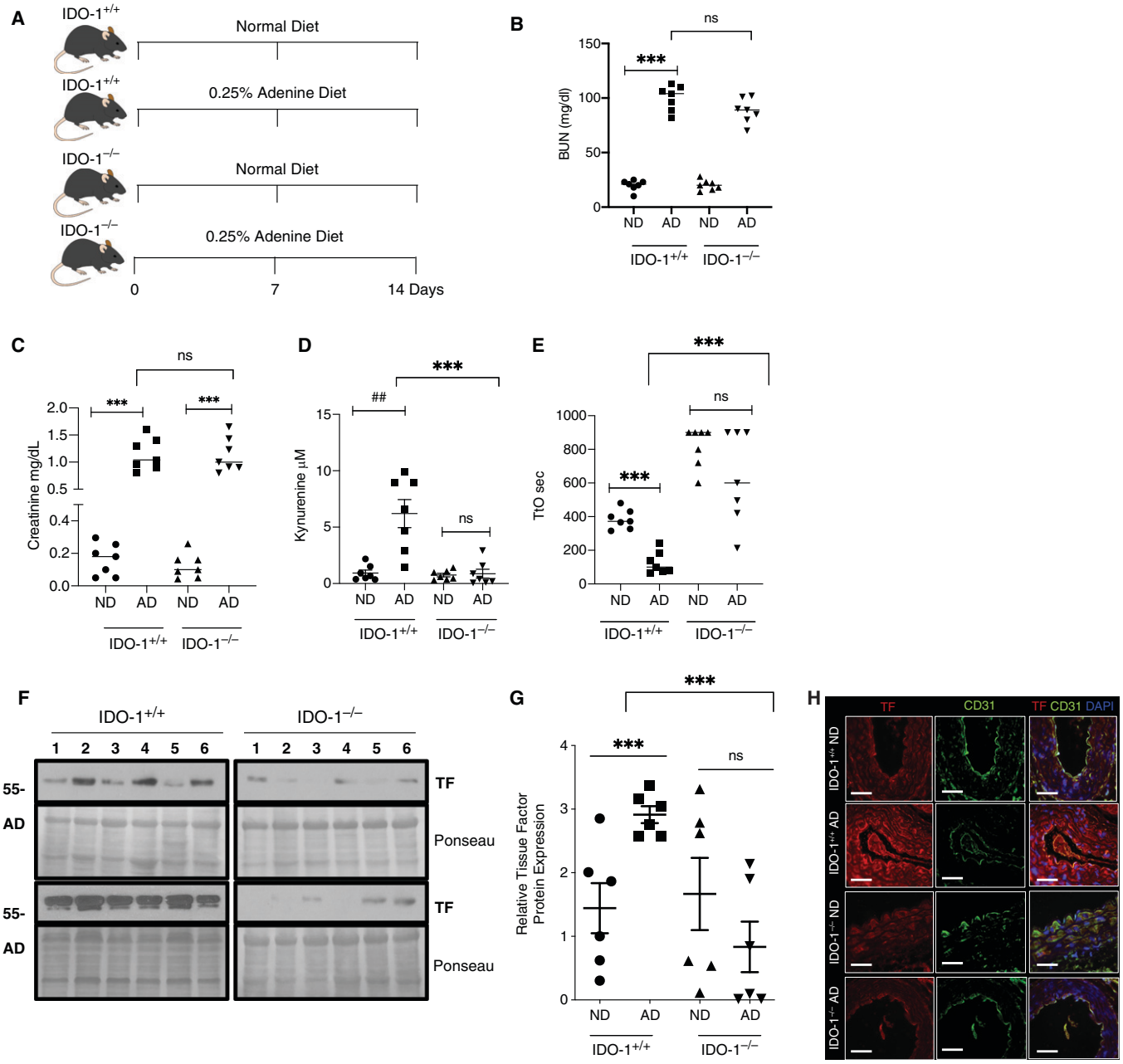

Figure 2. Global loss of IDO-1 suppresses post-vascular injury thrombosis in CKD mice. (A) Experimental design. A group of 8-10-week-old female IDO$^{+/+}$ and IDO-1$^{-/-}$ mice on a C57BL/6 background were subjected to a normal diet or a 0.25% adenine diet for 14 days. Mice underwent a $FeCl_3$ model of carotid artery injury (n=7 mice per group).(B) Average BUN levels (mg/dl) of IDO$^{+/+}$ and IDO$^{-/-}$ with and without a 0.25% adenine supplemented diet from (A) are shown. ANOVA was P<0.001. Student's t test was applied to compare the individual group. ns = no significant difference. ***P<0.001. n=7 mice per group. Error bars = SEM. (C) Average creatinine (mg/dl) of IDO$^{+/+}$ and IDO$^{-/-}$ mice with and without a 0.25% adenine supplemented diet are shown. ANOVA showed P<0.001. Student's t test was applied to compare the individual group. ***P<0.001. n=7 mice per group. Error bars = SEM. (D) Average Kyn in sera of the mice from (A) are shown. ANOVA was applied, which showed P<0.001. Student's t test was applied to compare the individual group. ***P<0.001 for Kyn between IDO-1$^{+/+}$ and IDO-1$^{-/-}$ CKD mice. $^{\#\#}P$=0.001 for Kyn levels in IDO-1$^{+/+}$ mice on normal and adenine diet. n=7 mice per group. Error bars = SEM. (E) Average TtO of thrombosis of the carotid artery of IDO$^{+/+}$ and IDO$^{-/-}$ mice with and without a 0.25% adenine supplemented diet included in (A) are shown. ANOVA was applied followed by Tukey's post-test (Supplemental Table 3). Error bars = SEM. ***P corresponds to significant difference. (F) Mice in the indicated group were exposed to a 0.25% adenine diet and harvested after 14 days. Mice on normal diet served as controls. Their aortic lysates were probed for TF. Ponseau served as controls. Immunoblots of six mice are shown. (G) Densitometry analysis was

0.93±0.25 μM and adenine diet 6.25±1.24 μM, P=0.001) (Figure 2D), consistent with previous observations.[21,42] This upregulation was significantly reduced (close to non-CKD levels) in IDO- $1^{-/-}$ CKD mice (0.75±0.15 μM) compared with IDO-$1^{+/+}$ CKD mice (P=0.002). Interestingly, the levels of serum Kyn were similar between IDO-$1^{+/+}$ and IDO-$1^{-/-}$ mice on a normal diet. These data suggested that at baseline, IDO-1 contributed less to Kyn levels, possibly compensated by other IDO-1 isoforms (IDO-2 and TDO) to maintain the basal levels of Kyn. Similar Kyn levels between IDO-$1^{-/-}$ CKD mice and IDO-$1^{-/-}$ non-CKD mice suggested that IDO-1 is the predominant enzyme contributing to Kyn levels in the CKD milieu.

Next, TtO was compared among different groups. Given multiple comparisons, ANOVA followed by Tukey's multiple pairwise comparisons were performed (Supplemental Table 3). IDO-$1^{+/+}$ CKD mice had a significantly shorter TtO (125.7±25.29 sec) compared with IDO-$1^{+/+}$ mice on a normal diet (384.3±21.86 sec, P<0.001), consistent with the effect of CKD observed in the past[20] (Figure 2E). IDO-$1^{-/-}$ mice on a normal diet had TtO (817.1±44.81 sec), which was significantly increased compared with both IDO-$1^{+/+}$ mice on a normal diet (384.3±21.86 sec) and IDO-$1^{+/+}$ mice on an adenine diet (125.7±25.29 sec). There was no difference in TtO in IDO-$1^{-/-}$ mice between normal (817.1±44.81 sec) and CKD diet (632.6±104.2 sec). There was a two-fold increase in TtO between IDO-$1^{-/-}$ mice and IDO-$1^{+/+}$ mice on normal diet. However, the extent of increase in TtO was greater (five-fold) between IDO-$1^{-/-}$ mice and IDO-$1^{+/+}$ mice on adenine diet.

Because TF in the vSMCs is a driver of thrombosis after vascular injury,[47] we next examined TF expression in the aorta of IDO-$1^{+/+}$ and IDO-$1^{-/-}$ mice on a normal or 0.25% adenine diet for 14 days. Ponceau staining served as a loading control. These mice did not undergo chemical injury, as this trauma is likely to modulate TF expression. Our results revealed an approximately two-fold increase in TF expression in the aorta of IDO-$1^{+/+}$ CKD mice, compared with IDO-$1^{+/+}$ mice on a normal diet. This is consistent with our previous observation.[17–20] TF expression in IDO-$1^{-/-}$ mice on an adenine diet was three-fold lower than IDO-$1^{+/+}$ mice on adenine diet, suggesting that global IDO-1 knock out downregulated TF expression in the aorta (Figure 2, F and G). These results are consistent with prolonged TtO in these mice. We further validated these findings using a double-label IF assay, where mice aortas were stained with TF, CD31, and SMA antibodies. Our results showed an increase in TF expression in the endothelial cells and vSMCS of IDO-$1^{+/+}$ mice on an adenine diet compared with IDO-$1^{+/+}$ mice on a normal diet. IDO-$1^{-/-}$ mice showed minimal baseline TF level in mice on a normal diet, and no increase in CKD mice (Figure 2H). Collectively, all of the above data suggested that global KO of IDO-1 downregulated TF expression in the arteries of mice and abrogated the hyperthrombotic milieu in CKD mice.

IDO-1 Inhibitors Decrease TF Expression in vSMCs

The above data examined *in vivo* TF regulation with genetic manipulation of IDO-1. IDO-1 inhibitors are in clinical trials for cancer therapeutics.[48] We used a panel of competitive inhibitors of IDO-1 (Supplemental Table 2) on the basis of their IC50 for IDO-1 inhibition.[48] Primary human aortic vSMCs were cotreated with uremic serum obtained from patients with ESKD receiving treatment with hemodialysis (baseline characteristics described previously[18]) and increasing concentrations of IDO-1 inhibitors (Figure 3). In parallel, vSMCs treated with the control serum served as controls (Supplemental Figure 3). Cotreatment with uremic sera and 1-MT downregulated TF expression <28.33% compared with vSMCs treated with uremic sera alone (Figure 3, A and B). Similarly, other IDO-1 inhibitors, such as indoximod (NLG8189) and NLG919, decreased TF expression in vSMCs cotreated with 5% uremic sera by 25%–38.2%, compared with vSMCs with 5% uremic sera alone (Figure 3, C–H). The highest uremic serum-induced TF suppression was observed with INCB23460. None of the IDO-1 inhibitors showed suppression of TF in vSMCs in the presence of control serum, but rather there was a nonsignificant trend toward TF upregulation upon treatment with IDO-1 inhibitors in the presence of control serum. These data suggested that pharmacologic manipulations of IDO-1 downregulated TF specifically in response to the uremic serum in vSMCs.

Inhibition of IDO-1 with 1-MT Decreases Thrombogenicity in a Mouse Model of CKD

Because TF in vSMCs is the primary driver of post-injury thrombosis[47] and is suppressed by IDO-1 inhibitors in vSMCs in CKD, we examined the effects of pharmacological manipulation of IDO-1 in a mouse model of CKD. IDO$^{+/+}$ mice pretreated with twice-daily intraperitoneal injections of 1-MT (50 mg/kg) for 2 days before starting the 0.25% adenine diet and were then subjected to the $FeCl_3$-induced carotid artery injury

Figure 2. (*Continued*) performed using ImageJ on TF bands using Ponseau as a loading control. Average normalized TF from six different mice exposed to normal and adenine diet is shown. ANOVA was P<0.001. Student's t test with Welch's correction was performed to compare few groups. ***P=0.005 between IDO-$1^{+/+}$ CKD mice and IDO-1+/+ mice on normal diet. ***P=0.006 between IDO-$1^{+/+}$ CKD mice and IDO-$1^{-/-}$ CKD mice. No difference in TF was found between IDO-$1^{-/-}$ CKD mice and IDO-$1^{-/-}$ mice on a normal diet (ns). (H) Aorta from mice exposed to a 0.25% adenine diet or a normal diet for 14 days were stained with IDO-1 and DAPI as indicated. CD31 and SMA served as markers of endothelial cells and vSMCs, respectively. Images obtained at 600× magnification from six independent mice per group are shown. Scale bars = 100 μM for CD31 and 30 μM for SMA.

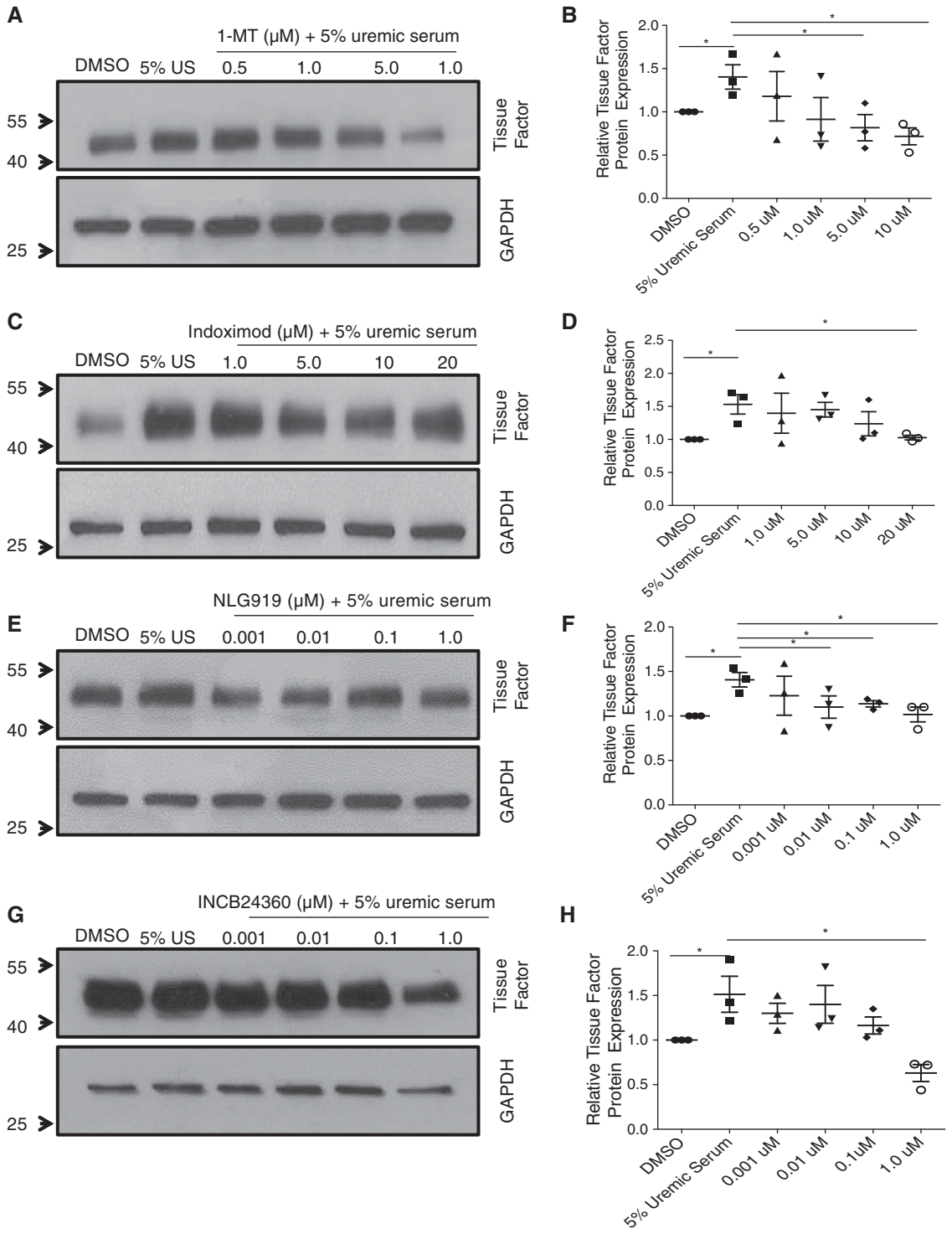

Figure 3. A panel of preclinical IDO-1 inhibitors suppress uremic-serum induced TF in primary human aortic vSMCS. (A), (C), (E), and (F) Representative immunoblots of lysates of primary human aortic vSMCs cotreated with 5% pooled uremic sera and increasing concentrations of the IDO-1 inhibitor and probed for TF. The concentrations of IDO-1 inhibitors were selected on the basis of their known IC50 for IDO-1 inhibition. GADPH served as a loading control ($n=3$ independent experiments). (B), (C), (F), and (G) Quantification of TF band normalized to GAPDH using ImageJ. Data presented as fold-change compared with DMSO-treated controls. Bars represent the average of three independent experiments. Error bars = SEM. ANOVA and Student's *t* test were performed. *$P<0.05$.

(Figure 4A). Vehicle-treated mice on the 0.25% adenine diet served as controls. In total, 4 days of the adenine diet was sufficient to increase BUN by approximately 3.5-fold from 21.07±2.720 mg/dl compared with 78.34±3.923 mg/dl (P=0.002). No difference in BUN was noted between the 1-MT–treated group and vehicle-treated CKD mice (Figure 4B). Histologic analysis of hematoxylin and eosin–stained kidney tissue showed patchy loss of tubular brush border, tubular damage, and wider tubular lumen (white asterisk, Figure 4C) to a comparable extent in both the groups. TtO of control mice was 274.8±10.35 s compared with mice with 1-MT 350.0±15.07 s (P=0.008) (Figure 4D). Further, this increase in TtO corresponded to a significant (approximately 50% reduction) in plasma Kyn (P=0.02) (Figure 4E), and a 40% reduction in TF expression in the aorta of 1-MT–treated mice compared with controls (P=0.008, Figure 4, F and G). These data suggested that IDO-1 inhibitor reduced thrombogenicity *in vivo* in a CKD model.

IS and Uremic Milieu Upregulate IDO-1 Expression in Vasculature

Because IS is known to upregulate TF in vSMCs and thrombosis[17,49] and IDO-1 regulated TF (Figures 2 and 3), we posited that IS may upregulate IDO-1 in vSMCs. To that end, we examined a prevalidated IS-specific solute model.[20] In this model, blood levels of IS are raised to levels corresponding to those present in patients with ESKD by increasing IS intake and inhibiting its excretion using probenecid, an OAT1 inhibitor.[29] A group of C57BL/6 mice were treated with twice-daily intraperitoneal injections of probenecid (150 mg/kg) with or without IS (4 mg/ml), *ad libitum*, through drinking water (Figure 5A). This model resulted in a 10-fold increase in the plasma IS concentration (P=0.03) (Figure 5B). Mice that received IS showed a close to 70% increase in IDO-1 protein expression in the aorta compared with the control mice (Figure 5, C and D). Our IHC analysis revealed that IDO-1 expression was increased in the medial layer of aorta with vSMCs and more prominently in the endothelial cells (asterisk and a black arrow, respectively, in Figure 5E) of the IS-treated mice. A 60% upregulation of IDO-1 was observed in the aorta of IS-exposed mice compared with probenecid control mice (Figure 5F).

We further examined these findings in an adenine-induced CKD model. Aortas derived of mice exposed to a normal or 0.25% adenine diet for 14 days were stained for IDO-1 and specific cellular markers, CD31 and SMA. The IF assay confirmed IDO-1 expression in endothelial cells and vSMCs of mice on a normal diet. IDO-1 expression was increased in both the cell types in CKD mice. The extent of the increase of IDO-1 seemed greater in vSMCs compared with endothelial cells (Figure 5, G and H). Collectively, these data suggested that IS and uremic milieu upregulated IDO-1 expression in the vessel wall.

IS Inhibits Polyubiquitination and Proteasomal Degradation of IDO-1

IDO-1 protein expression can increase due to mRNA induction or reduced protein degradation. Our analysis from the aorta showed that compared with controls, IS-treated mice had no differences in the ΔCt value for IDO-1 mRNA in the aortic lysates (ΔCt control=23.31 and ΔCt treated=23.14), suggesting IS exerted its effects on IDO-1 at the post-translational level. IS is known to modulate polyubiquitination and proteasomal degradation of proteins.[19,20] Polyubiquitinated proteins are detected in cells on blocking their proteasomal degradation with MG132. We first examined whether IDO-1 undergoes polyubiquitination in HEK-293T cells overexpressing IDO-1. Immunoprecipitated IDO-1 showed a 6–7-fold higher smear in the presence of MG132, suggesting IDO-1 undergoes polyubiquitination (Figure 6, A and B). We next examined if IS downregulated IDO-1 ubiquitination. HEK-293T cells expressing Flag-IDO were cotreated with IS at concentrations corresponding to patients with advanced CKD (50 μM). IS resulted in a six-fold reduction in the polyubiquitination of IDO-1 compared with the vehicle-treated cells (Figure 6, C and D). These data were confirmed in primary human aortic vSMCS, whereas IS treatment resulted in a 3.74-fold decrease in the ubiquitination of endogenous IDO-1 (Figure 6, E and F). These data suggested that IS suppressed polyubiquitination of IDO-1 and corroborated with the increased IDO-1 expression in the aorta of IS-treated mice or CKD mice (Figure 5, F and H).

Blood IDO-1 Activity Are Higher in Patients with Post-Vascular Injury Thrombosis

Upregulation of the protein IDO-1 is likely to correlate with increase in its activity, thus, augmenting the conversion of Trp to Kyn. Accordingly, a ratio of levels of Kyn/Trp in the blood is considered to reflect global IDO-1 activity and is used in different human studies.[50,51] We posited that IDO-1 activity is likely to be higher in patients with CKD and thrombosis. Given the focus on post-vascular injury thrombosis in this work, two clinical trials with post-interventional thrombosis as an end point were selected to examine this hypothesis. The DAC-Fistula trial[35] examined thrombosis within 6 weeks of AVF creation. In general, AVF thrombosis is a complex process driven, among other factors, by anastomotic or venous outflow stenosis, *etc.*[52–53] The study evaluated early thrombosis after AVF surgery, an event driven, at least in part, by injury to the endothelial layer during vascular surgery.[52–55] Also, examining AVF thrombosis within a short time period after AVF creation avoids confounders, such as outflow stenosis (inducing thrombosis by sluggish flow), which typically occur at a later time point after AVF creation. The TIMI-II trial[57] examined coronary artery thrombosis within 48 hours of balloon angioplasty (after endovascular intervention

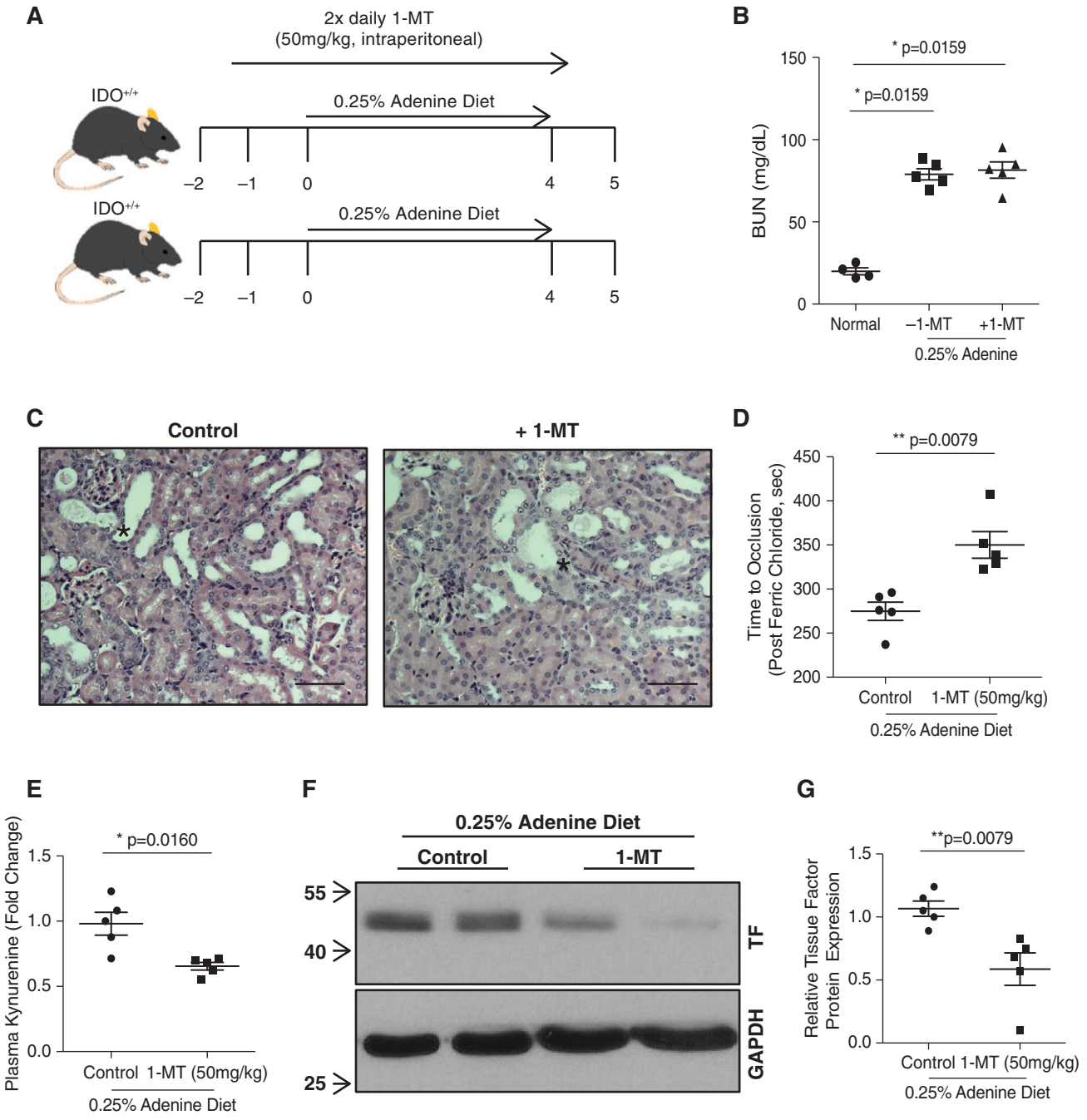

Figure 4. Pharmacological inhibition of IDO-1 downregulated TF expression and suppressed thrombogenicity in an adenine-induced CKD model. (A) Experimental design. Groups of IDO$^{+/+}$ C57/Bl6 mice were administered 0.25% adenine diet (n=5) with or without daily intraperitoneal injections of 1-MT (50 mg/kg intraperitoneal injections) (n=5 mice per group) as per the indicated protocol. (B) Average BUN at the end of experiments depicted in (A) is shown. n=5 mice per group. Student's t test was performed. Error bars = SEM. (C) Paraffin-embedded sections of kidneys of mice from both groups were stained with hematoxylin and eosin. Loss of tubular atrophy (marked with an asterisk), interstitial infiltrate and patch interstitial fibrosis indicate renal damage. 200× magnification, scale bar = 50 μM. (D) Average TtO in mice from both the groups of mice in (A) is shown. Student's t test was performed. Error bars = SEM. (E) Relative levels of plasma Kyn of mice depicted in (A) was normalized to control IDO$^{+/+}$ mice and presented as fold-change. Student's t test was performed. Error bars = SEM. (F) Aortic lysates from mice from both the groups were probed with TF antibody and GAPDH served as a loading control. Two representative aortic lysates from each group are shown (n=5 per group). (G) Quantification of TF expression normalized for GAPDH in the aorta of mice with and without 1-MT was performed using ImageJ. Data are presented as a fold change in normalized TF compared with control mice. Student's t test was performed. Error bars = SEM.

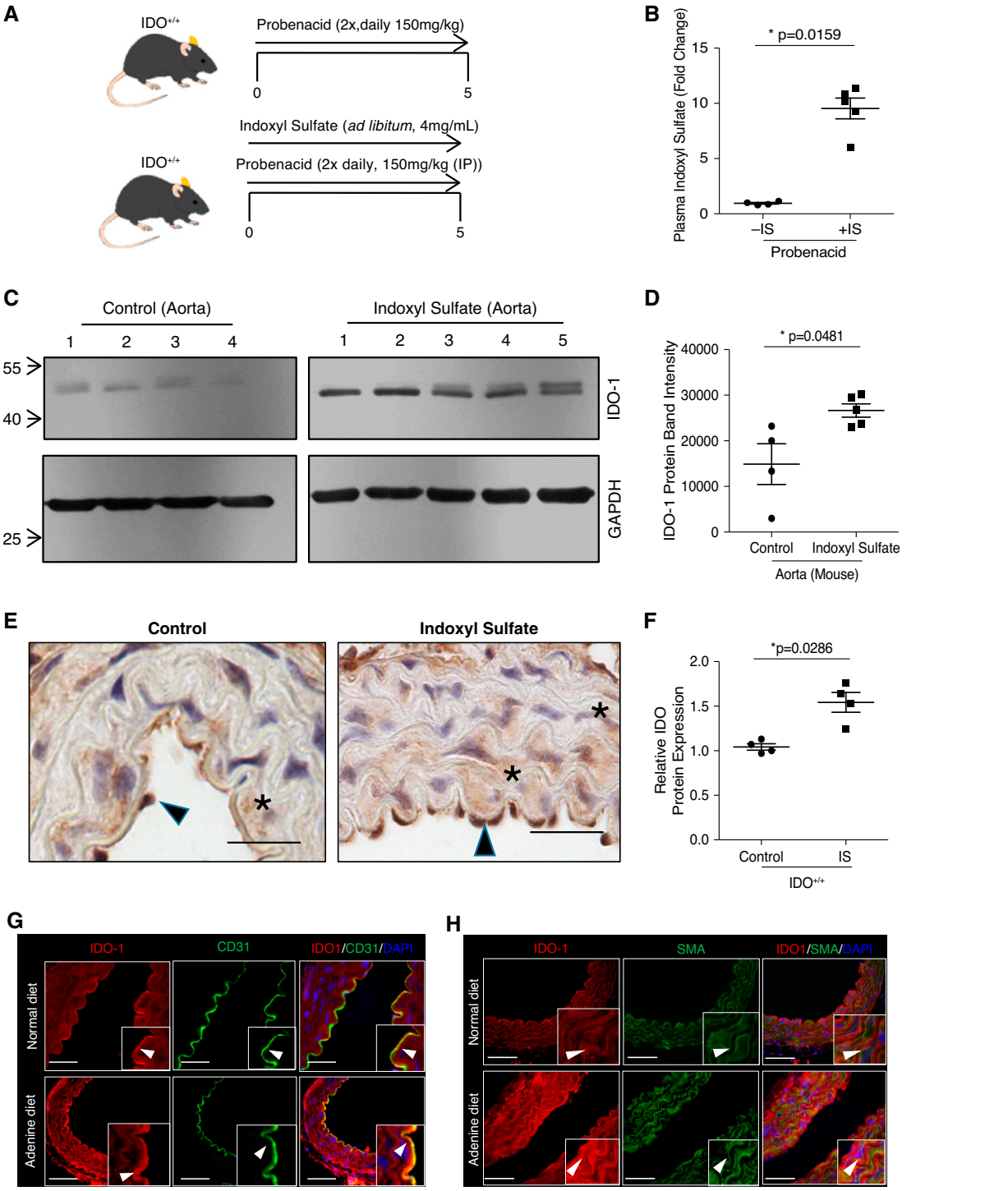

Figure 5. IS and CKD milieu increase IDO-1 protein in the aorta. (A) Experimental design of IS-solute specific model. IDO$^{+/+}$ mice were administered 150 mg/kg (intraperitoneally) probenecid twice daily (n=4) served as controls. The second group of IDO$^{+/+}$ mice were administered probenecid along with IS through drinking water *ad libitum* (4 mg/ml) for 4 days (n=5). (B) Relative levels of plasma IS of mice depicted in (A) was normalized to probenecid control mice and presented as fold-change. Student's *t* test was performed. Error bars = SEM. (C) Aortic lysates of mice depicted in (A) (numbered above the TF blot) from both groups were probed for IDO-1. GAPDH served as a loading control. (D) Quantification of IDO-1 expression normalized for GAPDH in the aorta of mice from both the groups was performed using ImageJ. Data are presented as a fold change in normalized TF compared with control mice. Student's *t* test was performed. Error bars = SEM. (E) Aortas of mice exposed to IS were stained for IDO-1 and counterstained with hematoxylin. Black arrow point to the endothelial cells in the intimal layer and the black asterisks are in the medial layer

thrombosis) in the setting of myocardial infarction. Both of these studies are well suited to examine our hypothesis regarding post-vascular injury thrombosis area.

Baseline sera obtained before the initiation of interventions were analyzed for the levels of Trp and Kyn. IDO-1 activity was calculated by on their ratio of Kyn/Trp.[50,57] For the DAC-Fistula trial, serum samples from 470 participants were examined, 60 of whom had AVF thrombosis within 6 weeks of AVF creation surgery. Participants with thrombosis had concentrations of Trp and Kyn of 27.78+10.92 μM and 6.6+0.50 μM, respectively. Participants without AVF thrombosis had similar concentrations of Trp (27.92+12.19 μM), but close to three-fold lower levels of Kyn (2.2+1.14 μM) ($P<0.001$). IDO-1 activity was 3.52-fold higher in participants who subsequently developed AVF thrombosis compared with those without thrombosis ($P<0.0001$) (Figure 7A). In the TIMI-II cohort available for analysis, 35 participants developed postangioplasty thrombosis and 342 participants had no thrombotic events. Trp and Kyn concentrations among the TIMI-II participants with thrombosis were 37.78±16.12 μM and 3.18±2.51 μM, respectively, compared with Trp and Kyn concentrations of 38.47±12.98 μM and 2.10±1.02 μM, respectively, among those without thrombosis ($P<0.001$ for comparisons of Kyn). IDO-1 activity was higher in participants with postangioplasty thrombosis by two-fold ($P=0.002$) compared with those without thrombosis (Figure 7B). Taken together, these data suggested IDO-1 activity was higher in the blood of patients with CKD who developed thrombosis after endovascular intervention (angioplasty) or vascular surgery (AVF creation).

DISCUSSION

This study focuses on an underappreciated complication in patients with CKD—post-vascular injury thrombosis. Given the heavy CVD burden, these patients frequently undergo complex vascular procedures. A United States Renal Data System database analysis from 2004 to 2009 of 23,033 patients with CKD stage 5 showed that 12,473 patients (approximately 50% of patients with CKD stage 5) underwent revascularization for acute coronary syndrome including bypass and/or stenting.[58] Additional 9673 coronary interventional procedures were performed in the context of stable or incidental CAD detected during evaluation for renal transplant.[58] The analysis of TAXUS ARRIVE Registries consisting of 7492 patients revealed that CKD increased the risk of stent thrombosis by 7.32-fold,[11] which resulted in death in 23% of patients and 28% with ST-elevation myocardial infarction.[11] All these studies highlight the magnitude and effect of postinterventional thrombosis in patients with CKD.[4–15]

Injury from vascular procedures inflicts endothelial cell damage, resulting in the exposure of highly thrombogenic subendothelial vSMCs, which serve as a reactive vascular bed to initiate thrombogenesis with cellular elements including platelets and microparticles in blood, etc. (Figure 8A).[61,60] Trp metabolites such as IS and Kyn convert the endothelium with its natural anticoagulant property to a procoagulant state by increasing TF on its surface.[17] These metabolites also make vSMCs more procoagulant.[18–20] In combination, these events condition the vessel wall to trigger the extrinsic coagulation cascade on vascular injury. Along with the previous studies[17,19,20,22] and probing the upstream regulators of Kyn biogenesis, this work demonstrates the genetic loss or pharmacologic inhibition of IDO-1 activity downregulates TF in the arterial wall and reduces thrombogenicity in a mouse model of CKD. Specifically, IS upregulates IDO-1 expression in the vessel wall, which initiates a positive feedback loop. IS, through IDO-1, augments the generation of more Kyn. Both IS and Kyn activate the AHR-TF thrombosis axis perpetuating the uremic thrombotic milieu and enhancing the risk of thrombosis after vascular injury (Figure 8B). Overall, this work advances our understanding IDO-1 biology, and mechanistic understanding of uremic thrombosis, while defining a novel node in this intricate network of uremic toxins that is amenable to pharmacological manipulation.

IDO-1 is an inducible enzyme and is upregulated in models of chronic inflammation, such as inflammation-associated arthritis and allergic airway disease.[61] Therefore, it stands to reason that IDO-1 is upregulated in CKD, which is a proinflammatory condition.[62] Although IFN-γ is considered to be a potent inducer of IDO-1, IFN-γ production was significantly reduced in patients with CKD,[63] raising a possibility of other inducer(s) of IDO-1 in CKD. Our results in cell-based and IS-specific solute models suggest IS is an inducer of IDO-1 *via* post-translational regulation.

IDO-1 is pursued as a "hot" target in cancer therapeutics and several IDO-1 inhibitors are in clinical trials.[48,64] Although these compounds have undergone extensive human safety studies, they are not evaluated specifically in patients with CKD. Some of the IDO-1 inhibitors have

Figure 5. (*Continued*) consisting of vSMC. Representative images from four control and five mice exposed to IS are shown. Scale bar = 50 μM. (F) Quantification of IDO-1 in the aorta of IS-treated mice using ImageJ analysis. Data are represented as plus or minus SEM. Student's *t* test was performed. (G) Aorta from mice exposed to a 0.25% adenine diet or a normal diet for 14 days were stained with IDO-1 and DAPI as indicated. CD31 served as markers of endothelial cells. Images obtained at 600× magnification from six independent mice per group are shown. Inserts show endothelial cells with IDO-1 expression (marked by white arrowhead). Scale bar = 100 μM. (H) Aortas were stained as above with SMA and IDO-1. Representative images with 400× magnification from six different mice per group are shown. The inserts show a part of the aorta with SMA and IDO-1 (marked by white arrowhead). Scale bar = 30 μM.

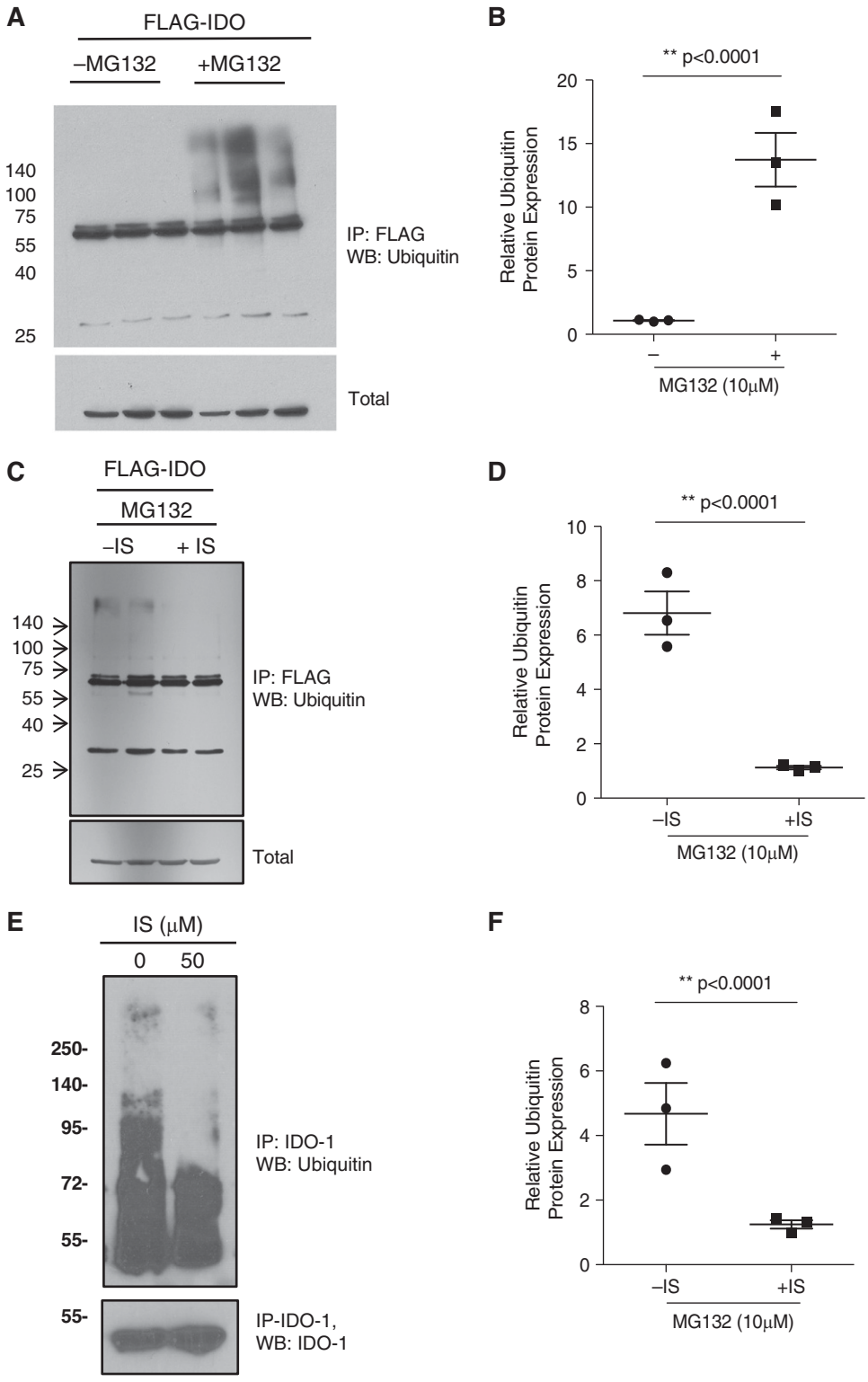

Figure 6. IS inhibits polyubiquitination and proteasomal degradation of IDO-1. (A) HEK-293T cells were transiently transfected with Flag-tagged IDO-1 and then treated with or without MG132 10 μM overnight before harvest. IDO-1 was immunoprecipitated using Flag-tag antibody, and the eluents were probed ubiquitin antibody. Representative image from three independent experiment performed in triplicate are shown. (B) Quantification of polyubiquitinated IDO-1 normalized to the total IDO-1. Data are represented as ±SEM. Student's *t* test was performed. (C) HEK-293T cells were transiently transfected with Flag-tagged IDO-1 and then treated

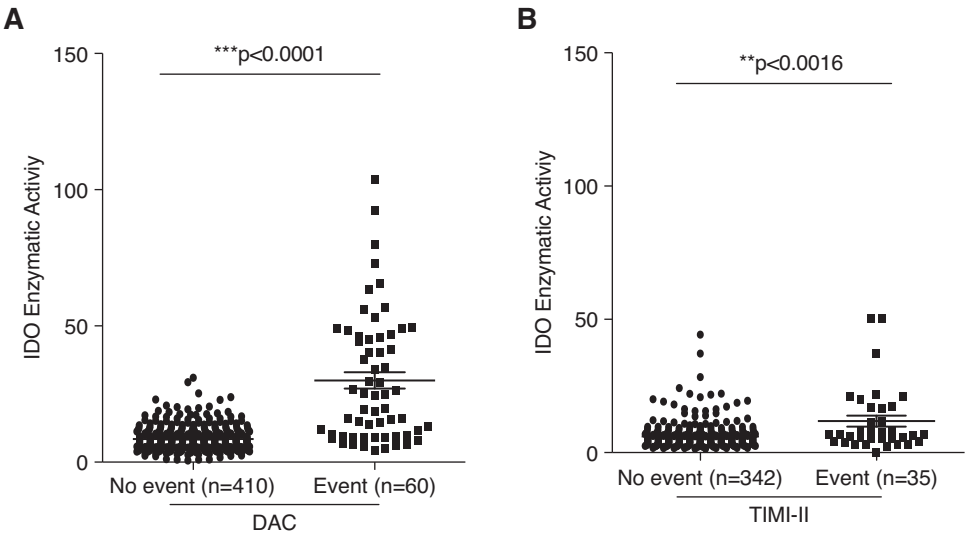

Figure 7. Increased IDO-1 activity in patients with CKD who subsequently developed post-vascular injury thrombosis. (A) IDO-1 activity in the baseline sera of participants in the DAC-Fistula trial was calculated as the ratio of blood levels of Kyn/Trp. Individual IDO-1 activity is shown in participants who subsequently developed arteriovenous fistula thrombosis (event); those without thrombosis (no event) served as controls. Student's *t* test was used for comparison. The line represents the median IDO-1 activity level. (B) IDO-1 activity in the baseline sera of the participants of TIMI-II trial was calculated as above and compared between those who subsequently developed postangioplasty thrombosis of coronary artery (event) and those without thrombosis (no events, controls). Student's *t* test was used for comparisons. The line represents the median IDO-1 activity level.

context-dependent off-target effects and can paradoxically activate AHR pathway detected in a non-CKD context due to their Trp-mimicking structure.[65] This event can explain a nonsignificant trend toward higher TF levels in cells treated with control sera. That these IDO-1 inhibitors consistently downregulate uremic serum-induced TF in vSMCs support- their antithrombotic application in patients with CKD. Also, their mechanism of action sets them apart from emerging orthogonal approaches targeting Kyn. Pegylated-kynurinase enzyme is proposed to systemically deplete Kyn and limit Kyn-based pathologies.[14,66] However, this approach suffers from a limitation because kynurinase will further increase other metabolites of Trp, such as anthranilic acid and quinolinic acid, both of which are associated with thrombosis in patients with CKD and may exacerbate uremic manifestations such as neurocognitive disease.[67] Because IDO-1 inhibitors suppress the first step of Kyn biogenesis, they will reduce the above downstream catabolites of Kyn.

Thrombosis is a dynamic process orchestrated by several cell types[61,68] including PMNs, platelets, red blood cells, microparticles, neutrophil extracellular traps. Although our work focused on vSMCs as the primary component of reactive vascular bed for thrombogenesis, more information is needed to understand alteration in IDO-1 in the above-listed components of thrombosis. Female mice were used in this study because the development and validation of the thrombosis assays were performed in them.[20] Further work is needed to expand this study, including probing the influence of sex on IDO-1 regulation in uremia, the role of other isoforms of IDO-1 (TDO and IDO-2) in uremic thrombosis, putative E3 ligase mediating IDO-1's modulation by IS, and relative contributions of IDO-1 in endothelial cells versus vSMCs in CKD-induced thrombosis using cell-type specific knock outs. The former cell type is relevant in CKD, because endothelial dysfunction is universal in patients with CKD and may be relevant in post-vascular injury thrombosis. For example, the closure of endothelial

Figure 6. (*Continued*) with 50 μM of IS or vehicle for 24 hours and MG132 10 μM overnight before harvest. IDO-1 polyubiquitination assay was performed as above. Representative images of three independent experiments performed are shown. (D) Quantification of polyubiquitinated IDO-1 normalized to the total IDO-1. Data are represented as ±SEM. Student's *t* test was performed. (E) Primary human aortic vSMCs were treated with 50 μM of IS for 16 hours and MG132 10 μM for 4 hours before harvest. Immunoprecipitated IDO-1 was probed with ubiquitin antibody. The blot was stripped and reprobed with IDO-1. Representative images of three independent experiment are shown. (F) Quantification of polyubiquitinated IDO-1 normalized to IDO-1. Data are represented as ±SEM. Student's *t* test was performed.

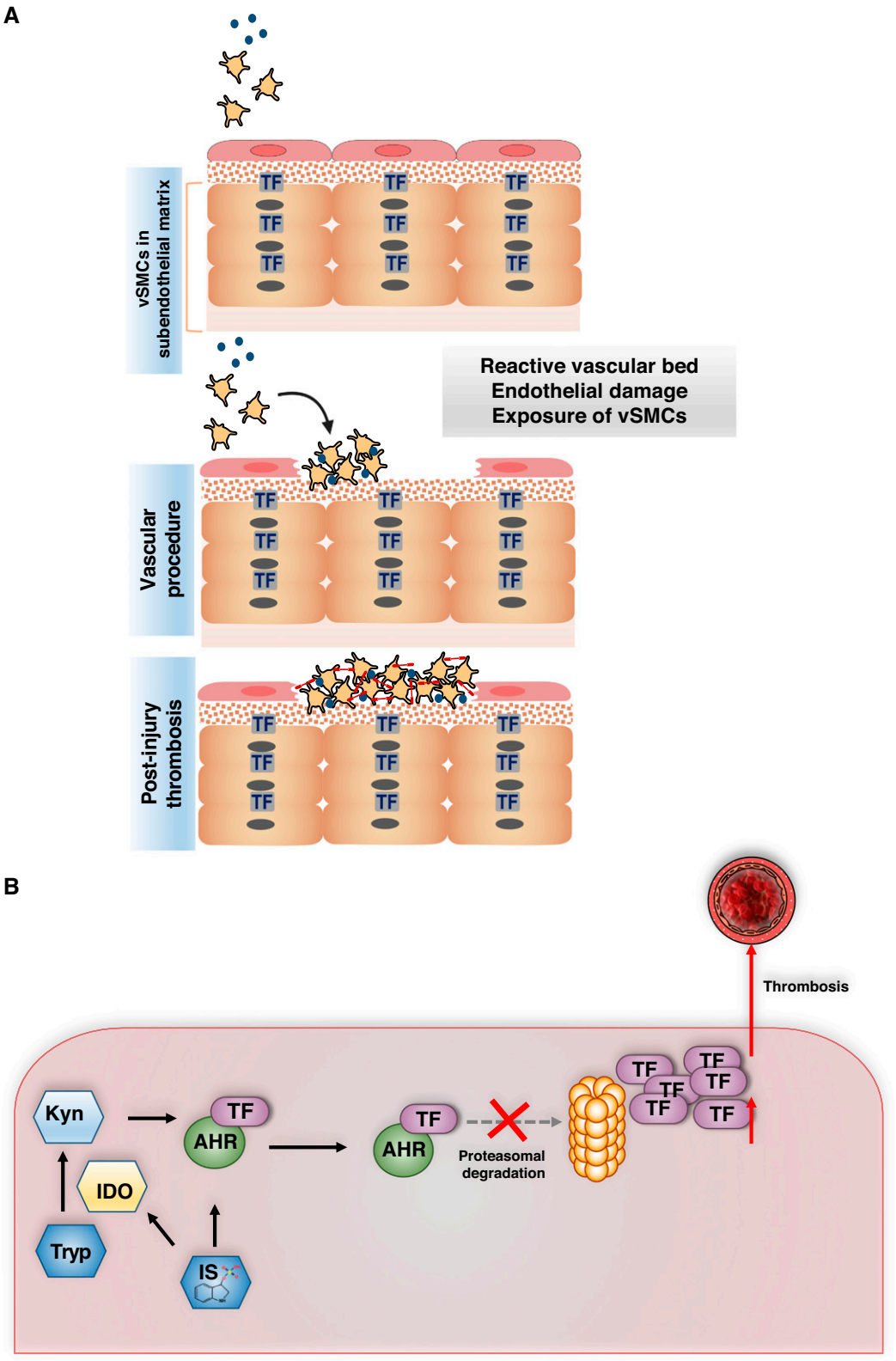

Figure 8. A model of post-vascular injury thrombosis and an interplay of uremic solutes exacerbating the hyperthrombotic CKD milieu. (A) Post-vascular injury thrombosis is an iatrogenic complication induced by vascular injury from endovascular procedures (angioplasty: coronary artery, peripheral artery or AVF; stenting *etc.*) and vascular surgery (coronary or fem-pop bypass or AVF

wounds inflicted by vascular procedures is critical to prevent thrombus extension.[59] It is conceivable that endothelial dysfunction results in poor healing of endothelial wounds, which then serves as a reactive bed for thrombus formation. This notion of poor reendothelialization in patients with CKD may explain the markedly higher risk of subacute (24 hours to 30 days) and chronic stent thrombosis (beyond 30 days) in patients with CKD.[3,8,10,11]

Hemodialysis is not able to effectively reduce the concentrations of protein-bound uremic toxins such as IS and Kyn. Therefore, inhibiting their synthesis (such as with IDO-1 inhibitors for Kyn) remains a viable option. Leveraging animal models and human data, this study paves a way to explore IDO-1 as a viable antithrombotic target in CKD.

DISCLOSURES

L. Dember reports receiving compensation from the National Kidney Foundation for her role as Deputy Editor; reports receiving consulting fees from AstraZeneca, Cara Therapeutics, and Merck; and reports fees to spouse from Actelion, Bristol Myers Squibb, Celgene, ChemoCentryx, Genentech/Roche, and GlaxoSmithKline. S. Richards reports being employed by Novartis Institute of Biomedical Research. V. Chitalia reports having consultancy agreements with Piramal Life Sciences and Senda Biosciences, Inc.; reports having an ownership interest in, and being a scientific advisor or member, of ConformationX Inc. and Orthogon Therapeutics Inc. All remaining authors have nothing to disclose.

FUNDING

This work was funded in part by the National Cancer Institute R01CA175382, NIH R01 HL132325 and Evans Faculty Merit award (to V. Chitalia), NHLBI R01HL136363 and NIH R01HL080442 (to K. Ravid), American Heart Association CAT-HD Center grant 857078 (VCC and SL), T32 training grant in cardiovascular biology T32 HL007224-40 (to J. Walker), T32 training grant in immunobiology of trauma T32 GM086308-06A1 (to N. Arinze), and the Thrombosis to Hemostasis in Health and Disease Affinity Research Collaborative (Boston University, Evans Center For Interdisciplinary Biomedical Research).

ACKNOWLEDGMENTS

V. Chitalia and K. Ravid conceptualized the hypothesis and J. Walker expanded it; V. Chitalia and J. Walker designed the experimental plan; K. Ravid provided critique and valuable insight; L. Dember provided insights related to the DAC-fistula study and interpretations of results; M. Belghasem, S.Lotfollahzadeh., S. Richards, and J. Walker performed *in vivo* animal experiments; M. Napoleon, S. Richards, T. Russell, J. Walker, and S.-B. Yoo performed the *in vitro* experiments; N. Lee and S. Whelan performed metabolomic analysis done by LC/MS; V. Chitalia and J. Walker prepared the manuscript; all authors edited the manuscript. We would like to thank Dr. Nigel Mackman (UNC, Chapel Hill) for guidance in TF antibody and IHC, and Dr. Michael Kirber and the Cellular Imaging Core at Boston University School of Medicine, Medical Campus for their help with imaging the histological experiments. We appreciate Prof. Janice Weinberg and Dr. Preya Patel (School of Public Health, BUSM) for the statistical support. We thank Dr. Grace (Qiong) Zhao (Department of Pathology, BUSM) for evaluation of organs of mice exposed to aden ine diet.

SUPPLEMENTAL MATERIAL

This article contains the following supplemental material online at http://jasn.asnjournals.org/lookup/suppl/doi:10.1681/ASN.2020091310/-/DCSupplemental.

Supplemental Materials and Methods.

Supplemental Figure 1. An adenine supplemented diet results in chronic kidney disease and increased incidence of thrombosis with elevated uremia in mice.

Supplemental Figure 2. Gross pathology of major organs with and without 0.25% adenine supplemented diet.

Supplemental Figure 3. IDO-1 inhibitors did not affect TF expression in smooth muscle treated with control serum.

Supplemental Table 1. Antibodies used and applications.

Supplemental Table 2. Competitive inhibitors of IDO-1.

Supplemental Table 3. Comparison of TtO in mice in different group using Tukey's multiple pairwise comparisons .

Supplemental References.

REFERENCES

1. Foley RN, Parfrey PS, Sarnak MJ: Clinical epidemiology of cardiovascular disease in chronic renal disease. *Am J Kidney Dis* 32: S112–S119, 1998
2. Ocak G, Rookmaaker MB, Algra A, de Borst GJ, Doevendans PA, Kappelle LJ, et al.; SMART Study Group: Chronic kidney disease and bleeding risk in patients at high cardiovascular risk: A cohort study. *J Thromb Haemost* 16: 65–73, 2018
3. Kimura T, Morimoto T, Kozuma K, Honda Y, Kume T, Aizawa T, et al.; RESTART Investigators: Comparisons of baseline demographics, clinical presentation, and long-term outcome among patients with early, late, and very late stent thrombosis of sirolimus-eluting stents: Observations from the Registry of Stent Thrombosis for Review and Reevaluation (RESTART). *Circulation* 122: 52–61, 2010
4. Motovska Z, Knot J, Widimsky P: Stent thrombosis: Risk assessment and prevention. *Cardiovasc Ther* 28: e92–e100, 2010
5. Park DW, Park SW, Park KH, Lee BK, Kim YH, Lee CW, et al.: Frequency of and risk factors for stent thrombosis after drug-eluting stent implantation during long-term follow-up. *Am J Cardiol* 98: 352–356, 2006

Figure 8. (*Continued*) creation, *etc.*). This event is triggered by endothelial damage, resulting in the exposure of highly thrombogenic subendothelial region consisting of vSMCs, which serve as a reactive vascular bed to initiate thrombogenesis. (B) The current data, along with previous studies, suggest that IS, a Trp-based uremic toxin, increases IDO-1 expression in endothelial cells and vSMCs. This event enhances Trp conversion to Kyn. An increase in Kyn, in turn, augments TF expression and thrombosis through AHR activation. Collectively, these studies support a model where IS upregulates the synthesis of another prothrombotic uremic solute, creating a feed-forward loop perpetuating the hyperthrombotic uremic milieu.

6. Fokkema ML, van der Vleuten PA, Vlaar PJ, Svilaas T, Zijlstra F: Incidence, predictors, and outcome of reinfarction and stent thrombosis within one year after primary percutaneous coronary intervention for ST-elevation myocardial infarction. *Catheter Cardiovasc Interv* 73: 627–634, 2009
7. Iakovou I, Schmidt T, Bonizzoni E, Ge L, Sangiorgi GM, Stankovic G, et al.: Incidence, predictors, and outcome of thrombosis after successful implantation of drug-eluting stents. *JAMA* 293: 2126–2130, 2005
8. Lambert ND, Sacrinty MT, Ketch TR, Turner SJ, Santos RM, Daniel KR, et al.: Chronic kidney disease and dipstick proteinuria are risk factors for stent thrombosis in patients with myocardial infarction. *Am Heart J* 157: 688–694, 2009
9. Ting, HH, Tahirkheli, NK, Berger, PB, McCarthy, JT, Timimi, FK, Mathew, V, Rihal, CS, Hasdai, D, Holmes, DR, Jr: Evaluation of long-term survival after successful percutaneous coronary intervention among patients with chronic renal failure. *Am J Cardiol* 87: 630–633, 2001
10. Szczech LA, Best PJ, Crowley E, Brooks MM, Berger PB, Bittner V, et al.; Bypass Angioplasty Revascularization Investigation (BARI) Investigators: Outcomes of patients with chronic renal insufficiency in the bypass angioplasty revascularization investigation. *Circulation* 105: 2253–2258, 2002
11. Lasala JM, Cox DA, Dobies D, Baran K, Bachinsky WB, Rogers EW, et al.; ARRIVE 1 and ARRIVE 2 Participating Physicians: Drug-eluting stent thrombosis in routine clinical practice: Two-year outcomes and predictors from the TAXUS ARRIVE registries. *Circ Cardiovasc Interv* 2: 285–293, 2009
12. Casserly LF, Dember LM: Thrombosis in end-stage renal disease. *Semin Dial* 16: 245–256, 2003
13. Shashar M, Francis J, Chitalia V: Thrombosis in the uremic milieu: Emerging role of "thrombolome". *Semin Dial* 28: 198–205, 2015
14. Ravid JD, Kamel MH, Chitalia VC: Uraemic solutes as therapeutic targets in CKD-associated cardiovascular disease. *Nat Rev Nephrol* 17: 402–416, 2021
15. Vanholder R, Schepers E, Pletinck A, Nagler EV, Glorieux G: The uremic toxicity of indoxyl sulfate and p-cresyl sulfate: A systematic review. *J Am Soc Nephrol* 25: 1897–1907, 2014
16. Mutsaers HA, Stribos EG, Glorieux G, Vanholder R, Olinga P: Chronic kidney disease and fibrosis: The role of uremic retention solutes. *Front Med (Lausanne)* 2: 60, 2015
17. Gondouin B, Cerini C, Dou L, Sallée M, Duval-Sabatier A, Pletinck A, et al.: Indolic uremic solutes increase tissue factor production in endothelial cells by the aryl hydrocarbon receptor pathway. *Kidney Int* 84: 733–744, 2013
18. Chitalia VC, Shivanna S, Martorell J, Balcells M, Bosch I, Kolandaivelu K, et al.: Uremic serum and solutes increase post-vascular interventional thrombotic risk through altered stability of smooth muscle cell tissue factor. *Circulation* 127: 365–376, 2013
19. Shivanna S, Kolandaivelu K, Shashar M, Belghasim M, Al-Rabadi L, Balcells M, et al.: The aryl hydrocarbon receptor is a critical regulator of tissue factor stability and an antithrombotic target in uremia. *J Am Soc Nephrol* 27: 189–201, 2016
20. Shashar M, Belghasem ME, Matsuura S, Walker J, Richards S, Alousi F, et al.: Targeting STUB1-tissue factor axis normalizes hyperthrombotic uremic phenotype without increasing bleeding risk. *Sci Transl Med* 9: 1–11, 2017
21. Karbowska M, Kaminski TW, Znorko B, Domaniewski T, Misztal T, Rusak T, et al.: Indoxyl sulfate promotes arterial thrombosis in rat model via increased levels of complex TF/VII, PAI-1, platelet activation as well as decreased contents of SIRT1 and SIRT3. *Front Physiol* 9: 1623, 2018
22. Pawlak K, Mysliwiec M, Pawlak D: Hypercoagulability is independently associated with kynurenine pathway activation in dialysed uraemic patients. *Thromb Haemost* 102: 49–55, 2009
23. Kolachalama VB, Shashar M, Alousi F, Shivanna S, Rijal K, Belghasem ME, et al.: Uremic solute-aryl hydrocarbon receptor-tissue factor axis associates with thrombosis after vascular injury in humans. *J Am Soc Nephrol* 29: 1063–1072, 2018
24. Meijers B, Evenepoel P, Anders HJ: Intestinal microbiome and fitness in kidney disease. *Nat Rev Nephrol* 15: 531–545, 2019
25. Bender DA: Biochemistry of tryptophan in health and disease. *Mol Aspects Med* 6: 101–197, 1983
26. Badawy AA: Tryptophan metabolism in alcoholism. *Nutr Res Rev* 15: 123–152, 2002
27. Badawy AA: Tryptophan availability for kynurenine pathway metabolism across the life span: Control mechanisms and focus on aging, exercise, diet and nutritional supplements. *Neuropharmacology* 112[Pt B]: 248–263, 2017
28. Capece L, Arrar M, Roitberg AE, Yeh SR, Marti MA, Estrin DA: Substrate stereo-specificity in tryptophan dioxygenase and indoleamine 2,3-dioxygenase. *Proteins* 78: 2961–2972, 2010
29. Dai X, Zhu BT: Indoleamine 2,3-dioxygenase tissue distribution and cellular localization in mice: Implications for its biological functions. *J Histochem Cytochem* 58: 17–28, 2010
30. Cuffy MC, Silverio AM, Qin L, Wang Y, Eid R, Brandacher G, et al.: Induction of indoleamine 2,3-dioxygenase in vascular smooth muscle cells by interferon-gamma contributes to medial immunoprivilege. *J Immunol* 179: 5246–5254, 2007
31. Beutelspacher SC, Tan PH, McClure MO, Larkin DF, Lechler RI, George AJ: Expression of indoleamine 2,3-dioxygenase (IDO) by endothelial cells: Implications for the control of alloresponses. *Am J Transplant* 6: 1320–1330, 2006
32. Bodary PF, Eitzman DT: Animal models of thrombosis. *Curr Opin Hematol* 16: 342–346, 2009
33. Cooley BC: Murine models of thrombosis. *Thromb Res* 129[Suppl 2]: S62–S64, 2012
34. Whinna HC: Overview of murine thrombosis models. *Thromb Res* 122[Suppl 1]: S64–S69, 2008
35. Dember LM, Beck GJ, Allon M, Delmez JA, Dixon BS, Greenberg A, et al.; Dialysis Access Consortium Study Group: Effect of clopidogrel on early failure of arteriovenous fistulas for hemodialysis: A randomized controlled trial. *JAMA* 299: 2164–2171, 2008
36. Terrin ML, Williams DO, Kleiman NS, Willerson J, Mueller HS, Desvigne-Nickens P, et al.: Two- and three-year results of the Thrombolysis in Myocardial Infarction (TIMI) Phase II clinical trial. *J Am Coll Cardiol* 22: 1763–1772, 1993
37. Yang HC, Zuo Y, Fogo AB: Models of chronic kidney disease. *Drug Discov Today Dis Models* 7: 13–19, 2010
38. Ali BH, Al-Salam S, Al Za'abi M, Waly MI, Ramkumar A, Beegam S, et al.: New model for adenine-induced chronic renal failure in mice, and the effect of gum acacia treatment thereon: Comparison with rats. *J Pharmacol Toxicol Methods* 68: 384–393, 2013
39. Claramunt D, Gil-Peña H, Fuente R, García-López E, Loredo V, Hernández-Frías O, et al.: Chronic kidney disease induced by adenine: A suitable model of growth retardation in uremia. *Am J Physiol Renal Physiol* 309: F57–F62, 2015
40. Jia T, Olauson H, Lindberg K, Amin R, Edvardsson K, Lindholm B, et al.: A novel model of adenine-induced tubulointerstitial nephropathy in mice. *BMC Nephrol* 14: 116, 2013
41. Walker JA, Richards S, Belghasem ME, Arinze N, Yoo SB, Tashjian JY, et al.: Temporal and tissue-specific activation of aryl hydrocarbon receptor in discrete mouse models of kidney disease. *Kidney Int* 97: 538–550, 2020
42. Bobeck E, Piccone ML, Bishop JW, Fulmer TG, Schwann DJ, et al.: Adenine-induced hyperphosphatemia in a murine model of renal insufficiency. *Nephrol Renal Dis* 2: 1–7, 2017
43. Gupta AK, Chopra BS, Vaid B, Sagar A, Raut S, Badmalia MD, et al.: Protective effects of gelsolin in acute pulmonary thromboembolism

and thrombosis in the carotid artery of mice. *PLoS One* 14: e0215717, 2019
44. Li P, Lin B, Tang P, Ye Y, Wu Z, Gui S, et al.: Aqueous extract of Whitmania pigra Whitman ameliorates ferric chloride-induced venous thrombosis in rats via antioxidation. *J Thromb Thrombolysis* 52: 59–68, 2020
45. Liu J, Cooley BC, Akinc A, Butler J, Borodovsky A: Knockdown of liver-derived factor XII by GalNAc-siRNA ALN-F12 prevents thrombosis in mice without impacting hemostatic function. *Thromb Res* 196: 200–205, 2020
46. Annarapu GK, Nolfi-Donegan D, Reynolds M, Wang Y, Shiva S: Mitochondrial reactive oxygen species scavenging attenuates thrombus formation in a murine model of sickle cell disease. *J Thromb Haemost* 19: 2256–2262, 2021
47. Taubman MB, Wang L, Miller C: The role of smooth muscle derived tissue factor in mediating thrombosis and arterial injury. *Thromb Res* 122[Suppl 1]: S78–S81, 2008
48. Prendergast GC, Malachowski WP, DuHadaway JB, Muller AJ: Discovery of IDO1 inhibitors: From bench to bedside. *Cancer Res* 77: 6795–6811, 2017
49. Kamiński TW, Pawlak K, Karbowska M, Myśliwiec M, Pawlak D: Indoxyl sulfate: The uremic toxin linking hemostatic system disturbances with the prevalence of cardiovascular disease in patients with chronic kidney disease. *BMC Nephrol* 18: 35, 2017
50. Schefold JC, Zeden JP, Fotopoulou C, von Haehling S, Pschowski R, Hasper D, et al.: Increased indoleamine 2,3-dioxygenase (IDO) activity and elevated serum levels of tryptophan catabolites in patients with chronic kidney disease: A possible link between chronic inflammation and uraemic symptoms. *Nephrol Dial Transplant* 24: 1901–1908, 2009
51. Umehara H, Numata S, Watanabe SY, Hatakeyama Y, Kinoshita M, Tomioka Y, et al.: Altered KYN/TRP, Gln/Glu, and Met/methionine sulfoxide ratios in the blood plasma of medication-free patients with major depressive disorder. *Sci Rep* 7: 4855, 2017
52. Roy-Chaudhury P, Kelly BS, Melhem M, Zhang J, Li J, Desai P, et al.: Vascular access in hemodialysis: Issues, management, and emerging concepts. *Cardiol Clin* 23: 249–273, 2005
53. Roy-Chaudhury P, Kelly BS, Miller MA, Reaves A, Armstrong J, Nanayakkara N, et al.: Venous neointimal hyperplasia in polytetrafluoroethylene dialysis grafts. *Kidney Int* 59: 2325–2334, 2001
54. Roy-Chaudhury, P, Spergel, LM, Besarab, A, Asif, A, Ravani, P: Biology of arteriovenous fistula failure. *J Nephrol* 20: 150–163, 2007
55. Farber A, Imrey PB, Huber TS, Kaufman JM, Kraiss LW, Larive B, et al.; HFM Study Group: Multiple preoperative and intraoperative factors predict early fistula thrombosis in the Hemodialysis Fistula Maturation Study. *J Vasc Surg* 63: 163–70.e6, 2016
56. TIMI Study Group: Comparison of invasive and conservative strategies after treatment with intravenous tissue plasminogen activator in acute myocardial infarction. Results of the thrombolysis in myocardial infarction (TIMI) phase II trial. *N Engl J Med* 320: 618-627, 1989
57. Hestad KA, Engedal K, Whist JE, Farup PG: The relationships among tryptophan, kynurenine, indoleamine 2,3-dioxygenase, depression, and neuropsychological performance. *Front Psychol* 8: 1561, 2017
58. Shroff GR, Solid CA, Herzog CA: Impact of acute coronary syndromes on survival of dialysis patients following surgical or percutaneous coronary revascularization in the United States. *Eur Heart J Acute Cardiovasc Care* 5: 205–213, 2016
59. Mackman N: Triggers, targets and treatments for thrombosis. *Nature* 451: 914–918, 2008
60. Grover SP, Mackman N: Tissue factor: An essential mediator of hemostasis and trigger of thrombosis. *Arterioscler Thromb Vasc Biol* 38: 709–725, 2018
61. Prendergast GC, Chang MY, Mandik-Nayak L, Metz R, Muller AJ: Indoleamine 2,3-dioxygenase as a modifier of pathogenic inflammation in cancer and other inflammation-associated diseases. *Curr Med Chem* 18: 2257–2262, 2011
62. Amdur RL, Feldman HI, Dominic EA, Anderson AH, Beddhu S, Rahman M, et al.; CRIC Study Investigators: Use of measures of inflammation and kidney function for prediction of atherosclerotic vascular disease events and death in patients with CKD: Findings from the CRIC Study. *Am J Kidney Dis* 73: 344–353, 2019
63. Lonnemann G, Novick D, Rubinstein M, Dinarello CA: Interleukin-18, interleukin-18 binding protein and impaired production of interferon-gamma in chronic renal failure. *Clin Nephrol* 60: 327–334, 2003
64. Hornyák L, Dobos N, Koncz G, Karányi Z, Páll D, Szabó Z, et al.: The role of indoleamine-2,3-dioxygenase in cancer development, diagnostics, and therapy. *Front Immunol* 9: 151, 2018
65. Günther J, Däbritz J, Wirthgen E: Limitations and off-target effects of tryptophan-related IDO inhibitors in cancer treatment. *Front Immunol* 10: 1801, 2019
66. Triplett TA, Garrison KC, Marshall N, Donkor M, Blazeck J, Lamb C, et al.: Reversal of indoleamine 2,3-dioxygenase-mediated cancer immune suppression by systemic kynurenine depletion with a therapeutic enzyme. *Nat Biotechnol* 36: 758–764, 2018
67. Bugnicourt JM, Godefroy O, Chillon JM, Choukroun G, Massy ZA: Cognitive disorders and dementia in CKD: The neglected kidney-brain axis. *J Am Soc Nephrol* 24: 353–363, 2013
68. Grover SP, Mackman N: Neutrophils, NETs, and immunothrombosis. *Blood* 132: 1360–1361, 2018

AFFILIATIONS

[1]Renal Section, Department of Medicine, Boston University School of Medicine, Boston, Massachusetts
[2]Whitaker Cardiovascular Institute, Boston University, Boston, Massachusetts
[3]Chemical Instrumentation Center, Boston University, Boston, Massachusetts
[4]Department of Surgery, Boston University School of Medicine, Boston, Massachusetts
[5]Department of Pathology and Laboratory Medicine, Boston University School of Medicine, Boston, Massachusetts
[6]Renal-Electrolyte and Hypertension Division, Center for Clinical Epidemiology and Biostatistics, Philadelphia, Pennsylvania
[7]Department of Biostatistics, Epidemiology and Informatics, Perelman School of Medicine at the University of Pennsylvania, Philadelphia, Pennsylvania
[8]Department of Medicine, Boston University School of Medicine, Boston, Massachusetts
[9]Veteran Affairs Boston Healthcare System, Boston, Massachusetts
[10]Institute of Medical Engineering and Science, Massachusetts Institute of Technology, Cambridge, Massachusetts

Supplementary Material Table of Contents:

Supplementary Materials and Methods:

Carotid artery injury model of vascular thrombosis:

For all animal models, following induction of CKD with an 0.25% adenine diet, thrombosis was analyzed using the carotid artery injury model of vascular thrombosis, as previously described[1]. Briefly, the right carotid artery was exposed following anesthesia with isoflurane. Baseline blood flow was recorded using a 0.5PSB S-Series flow probe connected to a TS420 perivascular transit-time flow meter (Transonic; Ithaca, NY.). The probe was removed and damage to the artery was performed by placing a piece of Whatman filter paper (1x3mm) soaked in 5% ferric chloride ($FeCl_3$) under it for 1 min. Following washing with physiological saline (0.9% sodium chloride, 37°C) blood flow was monitored and TTO was determined as the first measurement of blood flow <0.299 mL/min. If no clot developed, the assay was terminated after 15 min. Animals were sacrificed by cervical dislocation following blood collection from the carotid artery into heparin coated tubes. Animals were perfused with an excess of ice cold 1x PBS. Tissues were harvested and preserved in either 10% formalin or snap frozen on liquid nitrogen for subsequent analysis.

Animal tissue lysis and Immunoblot:

10-15mg of aorta was lyzed in 2% sodium dodecyl sulfate (SDS) with 5mM EDTA and 1mM sodium orthovanadate (Tissue lysis buffer). Tissue was mechanically homogenized and lysed using sonication with insoluble debris removed by centrifugation for 15min (13,000 RPM at 4°C). The supernatant was removed and protein concentration determined using a BCA protein assay (Pierce, cat# 23227) Lysates were resolved by electrophoresis on a 10% agarose gel before transferring to a 0.2µm nitrocellulose membrane (Bio-Rad, cat# 1620112) (1hr at 4°C). Membranes were cut and blocked in 5% non-fat milk for 1hr at room temperature (RT). Blots were incubated overnight at 4°C with primary antibodies (Table 1). GAPDH served as a loading control for all immunoblots. Following washing with 1x

TBS-T (3x, 10min), blots were incubated at RT for 1hr with an appropriately horseradish peroxidase (HRP) labeled secondary antibody and developed using Western HRP substrate (Millipore, cat# WBLUC0500). In the experiments with different groups and several samples in each group, all the samples could not be included on a single gel, which represents a limitation. However, all the bands were normalized to the loading control such as GAPDH or actin.

Immunohistochemistry:

Following sacrifice and perfusion of indoxyl sulfate treated animals, sections of the aorta from each mouse were fixed in 10% formalin, overnight, at 4°C before being processed and embedded in paraffin. 5 µM sections were deparaffinized in xylenes and rehydrated in decreasing concentrations of ethanol before antigen retrieval with a sodium citrate buffer with high heat for 20 mins. Following antigen retrieval, endogenous peroxidase was blocked and slides subsequently washed 2x in 1x TBS-T for 5mins. After blocking for 30mins with a serum free protein block, sections were incubated overnight with an anti-IDO antibody (Supplementary Table 1) at 4°C. Sections were washed 2x in 1x TBS-T before incubating with an appropriate horseradish peroxide (HRP) labeled secondary antibody. The color reaction was monitored under a microscope during incubation with 3, 3'-Diaminobenzidine (DAB), with the reaction stopped by incubating the sections in water. Sections were counterstained in hematoxylin, then dehydrated in increasing concentrations of ethanol and cleared in xylenes before mounting. Sections were imaged using a Nikon TE 2000 wide-field microscope at 200x magnification. Intensity of IDO-1 signal in the aorta was analyzed using ImageJ analysis by measuring the intensity along a line from the intima through the media layers of the aorta. Five line analyses were done per section for each of the control (n=4) and experimental animals that received indoxyl sulfate (n=5).

Immunofluorescence

Formalin-fixed, paraffin-embedded tissue blocks were sectioned at 4μM and subjected to a heat-induced antigen retrieval using 10mM sodium citrate, pH 6.0 for 20mins. Tissue sections were blocked with 1% BSA in 1x PBS containing 0.3% Triton X-100 for 30mins at room temperature. Tissue sections were subsequently incubated with primary antibodies or a corresponding isotype control overnight at 4°C. Following washes in 1x TBS-T, sections were incubated with corresponding Alexa Fluor 488 or 594 conjugated fluorescent secondary antibodies for 1hr at room temperature. Tissue sections were washed in 1x TBS-T before staining nucelli with DAPI, mounted with fluorescence mounting medium and cover slip. All sections were imaged using a Leica SP5 point-scan epifluorescence laser confocal microscope.

IDO-1 inhibitor treatment:

Primary human aortic vascular smooth muscle cells (VSMCs) (P5) were plated at a confluence of 50-60% in 6 well culture plates**.** Cells were grown in Dulbecco's Modified Eagle Medium (DMEM) (Gibco, cat# 11054-020) supplemented with 5% calf sera, glutamine, and penicillin/streptomycin (P/S). VSMCs were serum starved overnight in full media supplemented with 0.5% calf sera. Cells were co-treated with increasing concentrations of indoleamine 2,3-dioxygenase-1 (IDO-1) inhibitors (Table 2) for 24hr with 5% uremic sera. DMSO and 5% sera from control patients served as controls. Cells were lysed in 1x RIPA buffer (Boston Bioproducts, cat# BP-115). Protein concentrations were determined using a Bradford protein assay and insoluble debris pelleted as described above. Proteins were resolved on a 10% agarose gel and transferred to a nitrocellulose membrane as described above before immunoblotting with an antibody raised against human Tissue Factor as described above.

Indoxyl Sulfate-Solute Specific Model

Twelve week old C57/BL6J mice were administered indoxyl sulfate (IS), *ad libitum*, through drinking water (4mg/mL). In order to simulate an increase in the IS similar to seen in patients with CKD,

excretion of IS was inhibited by twice daily injection of the organic anion transporter (OAT) inhibitor, probenecid (150mg/kg, intraperitoneal injection)[2]. Mice were administered this protocol for 4 days before sacrifice and perfusion with 1x ice cold PBS. The aorta was removed and lysed to determine the direct effects of IS on IDO-1 protein expression in endothelial and vascular smooth muscle cells.

Metabolomics/Mass Spec:

Metabolites, indoxyl sulfate and kynurenine, were measured using liquid chromatography/mass spectrometry (LC/MS) as previously described[2]. Briefly, sera samples were diluted 1:8 (sample: solvent) in an 8:1:1 mix of Acetonitrile:Methanol:Acetone and kept on ice for 30 mins to precipitate proteins and lipids. Proteins and lipids were pelleted by centrifugation at 15,000 rcf for 10 mins at <10^{o}C, followed by drying in a speed vacuum and reconstituted in 40µl µL H_20 with 0.1% formic acid and vortexed. Supernatant was transferred to a labeled glass LC vial with glass insert and placed into an Agilent HPLC 1100 series auto sampler.

For negative polarity detection of IS and Kyn a gradient of 95% H2O and 0.1% formic acid (buffer A) and 5% methanol (buffer B) at 0-0.5min, 95% buffer B at 5min, 98% buffer B at 8.5min, and 5% buffer B at 9.0- 10.0min at a flow rate of 0.15ml/min. A LTQ XL (Thermo Scientific) with an ESI source was used in negative mode with first event a full MS scan at 55.0-250.0m/z, isolation width 1.0, mass range normal, scan rate normal and data type profile. Scan event two was set to fragment indoxyl sulfate parent ion 212.0, CID activation with normalized collision energy 50.0, isolation width 3.0, activation Q at 0.25 and activation time of 30.0 ms. For positive polarity detection a gradient of 95% buffer A at 0.00-1.00min, 15% buffer B at 4.00min, 95% buffer B at 7.00-8.00 min, and 5% buffer B at 8.50-10.0min. In positive polarity mode the first full MS scan was at 55.0-500.0 m/z, isolation width 1.0, mass range normal, scan rate normal and data type profile. Scan event two was set to target kynurenine parent ion 209.00 m/z with a scan range of 55.0-225.0 m/z, CID activation with normalized collision energy 50.0,

isolation width 3.0, activation Q at 0.25 and activation time of 30.0 ms. Wideband activation was checked.

Supplementary Figure Legend

Supplementary Figure 1. An adenine supplemented diet results in chronic kidney disease and increased incidence of thrombosis with elevated uremia in mice

A. Experimental design. A group of female C57Bl/6 mice were fed a normal or 0.25% adenine supplemented for 14 days with thrombosis determined using a $FeCl_3$ model of vascular injury on the carotid artery (n=5 mice per group).

B. Histological examination of hematoxylin and eosin (H&E) stained kidneys showed a significant decrease in tubular mass (asterisk) as well as a glomeruli degeneration (arrow) compared to mice on a normal diet (200x magnification, scale bar=50 microns).

C. H&E stained sections from heart and liver were examined from mice after 14 days of a normal or 0.25% adenine supplemented diet. Gross changes to the kidney were observed in mice on an adenine supplemented diet with major findings being tubular degeneration, inflammation, and interstitial fibrosis. There were no gross differences between the heart and liver in mice on a normal diet compared to those on an adenine supplemented diet.

Supplementary Figure 2. Gross pathology of major organs with and without 0.25% adenine supplemented diet

A. Aortic lysates from mice on a normal diet or a 0.25% adenine diet for 14 days were probed with TF. GAPDH served as a loading control.

B. Quantification of TF band normalized to GAPDH was performed using ImageJ. There was a significant 1.65±0.14-fold increase in TF expression in the aorta of mice on an adenine diet for 14 days compared to mice on a normal diet (left, p=0.0301).

C. In mice on a 0.25% adenine diet, time to occlusion (TTO) was significantly decreased (p=0.0411) compared to mice on a normal diet, suggesting that with CKD there is an increase in thrombus formation with vascular injury**.**

Supplementary Figure 3. IDO-1 inhibitors did not affect Tissue Factor Expression in Smooth Muscle Treated with Control Serum

A-B. Primary human vascular smooth muscle cells were treated pooled control human serum obtained from subjected with normal renal function. Cells were treated with 5% control sera along with increasing concentrations of IDO-1 inhibitors. The lysates were probed for TF and HSP-90 served as loading controls. Representative images from three independent experiments are shown.

C-F. Quantification of TF expression was performed using ImageJ and normalized with HSP-90. Data is presented as an average and error bars = SEM.

Supplementary Table 1: Antibodies used and applications

Antibody	Company (Catalog Number)	Species Reactivity	Application	Dilution
GAPDH	Cell Signaling (#2118)	Mouse/Human	WB	1:1000
IDO, Clone 1F8.2	Millipore (#MAB10009)	Human	WB IHC	1:100 1:100
IDO, Clone 4B7	Millipore (#MABF850)	Mouse	WB IHC	1:100 1:100
CD142 (Tissue Factor)	BD Pharmigen (#550252)	Human	WB	1:2500
DYKDDDDK (FLAG)	Cell Signaling (#8146)	Mouse/Human	WB IP	1:1000 1µg/mL
Ubiquitin (P4D1)	Santa Cruz Biotechnology (sc-8017)	Human	WB	1:500

Supplementary Table 2: Competitive inhibitors of Indoleamine 2,3-Dioxygenase-1 (will have to get the references populating these numbers)

Compound	**Company (Catalog Number)**	**IC50**
NLG919	Medchem Express (HY-13983)	7nM
Indoximod	Medchem Express (HY-16724)	7µM
IDO5L	Medchem Express (HY-15683)	67nM
1-Methyl-L-Tryptophan	Enzo Life Sciences (ALX-106-040-M050)	7µM
INCB24360	Axon Medchem (2215)	10nM

Supplementary table 3. Comparison of TtO in mice in different group using Tukey's multiple pairwise comparisons

Group Comparison	Difference Between Means	Simultaneous 95% Confidence Limits		Significance
IDO-$1^{-/-}$ normal diet – IDO-$1^{-/-}$ Adenine	184.54	-46.07	415.16	
IDO-$1^{-/-}$ normal diet – IDO-$1^{+/+}$ normal diet	432.86	202.24	663.47	***
IDO-$1^{-/-}$ normal diet – IDO-$1^{+/+}$ Adenine	691.37	460.75	921.99	***
IDO-$1^{-/-}$ Adenine – IDO-$1^{-/-}$ normal diet	-184.54	-415.16	46.07	
IDO-$1^{-/-}$ Adenine – IDO-$1^{+/+}$ normal diet	248.31	17.70	478.93	***
IDO-$1^{-/-}$ Adenine – IDO-$1^{+/+}$ Adenine	506.83	276.21	737.45	***
IDO-$1^{+/+}$ normal diet – IDO-$1^{-/-}$ normal diet	-432.86	-663.47	-202.24	***
IDO-$1^{+/+}$ normal diet – IDO-$1^{-/-}$ Adenine	-248.31	-478.93	-17.70	***
IDO-$1^{+/+}$ normal diet – IDO-1 WT Adenine	258.51	27.90	489.13	***
IDO-$1^{+/+}$ Adenine – IDO-$1^{-/-}$ normal diet	-691.37	-921.99	-460.75	***
IDO-$1^{+/+}$ Adenine – IDO-$1^{-/-}$ Adenine	-506.83	-737.45	-276.21	***
IDO-$1^{+/+}$ Adenine - IDO-$1^{+/+}$ normal diet	-258.51	-489.13	-27.90	***

*** indicate significant p value.

Supplementary References

1. Matsuura S, Mi R, Koupenova M, et al. Lysyl oxidase is associated with increased thrombosis and platelet reactivity. *Blood*. 2016;127(11):1493-1501.

2. Walker JA, Richards S, Belghasem ME, et al. Temporal and tissue-specific activation of aryl hydrocarbon receptor in discrete mouse models of kidney disease. *Kidney Int*. 2020;97(3):538-550.

Supplementary Table 1: Antibodies used and applications

Antibody	Company (Catalog Number)	Species Reactivity	Application	Dilution
GAPDH	Cell Signaling (#2118)	Mouse/Human	WB	1:1000
IDO, Clone 1F8.2	Millipore (#MAB10009)	Human	WB IHC	1:100 1:100
IDO, Clone 4B7	Millipore (#MABF850)	Mouse	WB IHC	1:100 1:100
CD142 (Tissue Factor)	BD Pharmigen (#550252)	Human	WB	1:2500
DYKDDDDK (FLAG)	Cell Signaling (#8146)	Mouse/Human	WB IP	1:1000 1µg/mL
Ubiquitin (P4D1)	Santa Cruz Biotechnology (sc-8017)	Human	WB	1:500

Supplementary Table 2: Competitive inhibitors of Indoleamine 2,3-Dioxygenase-1 (will have to get the references populating these numbers)

Compound	**Company (Catalog Number)**	**IC50**
NLG919	Medchem Express (HY-13983)	7nM
Indoximod	Medchem Express (HY-16724)	7μM
IDO5L	Medchem Express (HY-15683)	67nM
1-Methyl-L-Tryptophan	Enzo Life Sciences (ALX-106-040-M050)	7μM
INCB24360	Axon Medchem (2215)	10nM

Supplementary table 3. Comparison of TtO in mice in different group using Tukey's multiple pairwise comparisons

Group Comparison	Difference Between Means	Simultaneous 95% Confidence Limits		Significance
IDO-$1^{-/-}$ normal diet – IDO-$1^{-/-}$ Adenine	184.54	-46.07	415.16	
IDO-$1^{-/-}$ normal diet – IDO-$1^{+/+}$ normal diet	432.86	202.24	663.47	***
IDO-$1^{-/-}$ normal diet – IDO-$1^{+/+}$ Adenine	691.37	460.75	921.99	***
IDO-$1^{-/-}$ Adenine – IDO-$1^{-/-}$ normal diet	-184.54	-415.16	46.07	
IDO-$1^{-/-}$ Adenine – IDO-$1^{+/+}$ normal diet	248.31	17.70	478.93	***
IDO-$1^{-/-}$ Adenine – IDO-$1^{+/+}$ Adenine	506.83	276.21	737.45	***
IDO-$1^{+/+}$ normal diet – IDO-$1^{-/-}$ normal diet	-432.86	-663.47	-202.24	***
IDO-$1^{+/+}$ normal diet – IDO-$1^{-/-}$ Adenine	-248.31	-478.93	-17.70	***
IDO-$1^{+/+}$ normal diet – IDO-1 WT Adenine	258.51	27.90	489.13	***
IDO-$1^{+/+}$ Adenine – IDO-$1^{-/-}$ normal diet	-691.37	-921.99	-460.75	***
IDO-$1^{+/+}$ Adenine – IDO-$1^{-/-}$ Adenine	-506.83	-737.45	-276.21	***
IDO-$1^{+/+}$ Adenine - IDO-$1^{+/+}$ normal diet	-258.51	-489.13	-27.90	***

*** indicate significant p value.

Supplementary References

1. Matsuura S, Mi R, Koupenova M, et al. Lysyl oxidase is associated with increased thrombosis and platelet reactivity. *Blood*. 2016;127(11):1493-1501.

2. Walker JA, Richards S, Belghasem ME, et al. Temporal and tissue-specific activation of aryl hydrocarbon receptor in discrete mouse models of kidney disease. *Kidney Int*. 2020;97(3):538-550.

Supplementary Figure 1

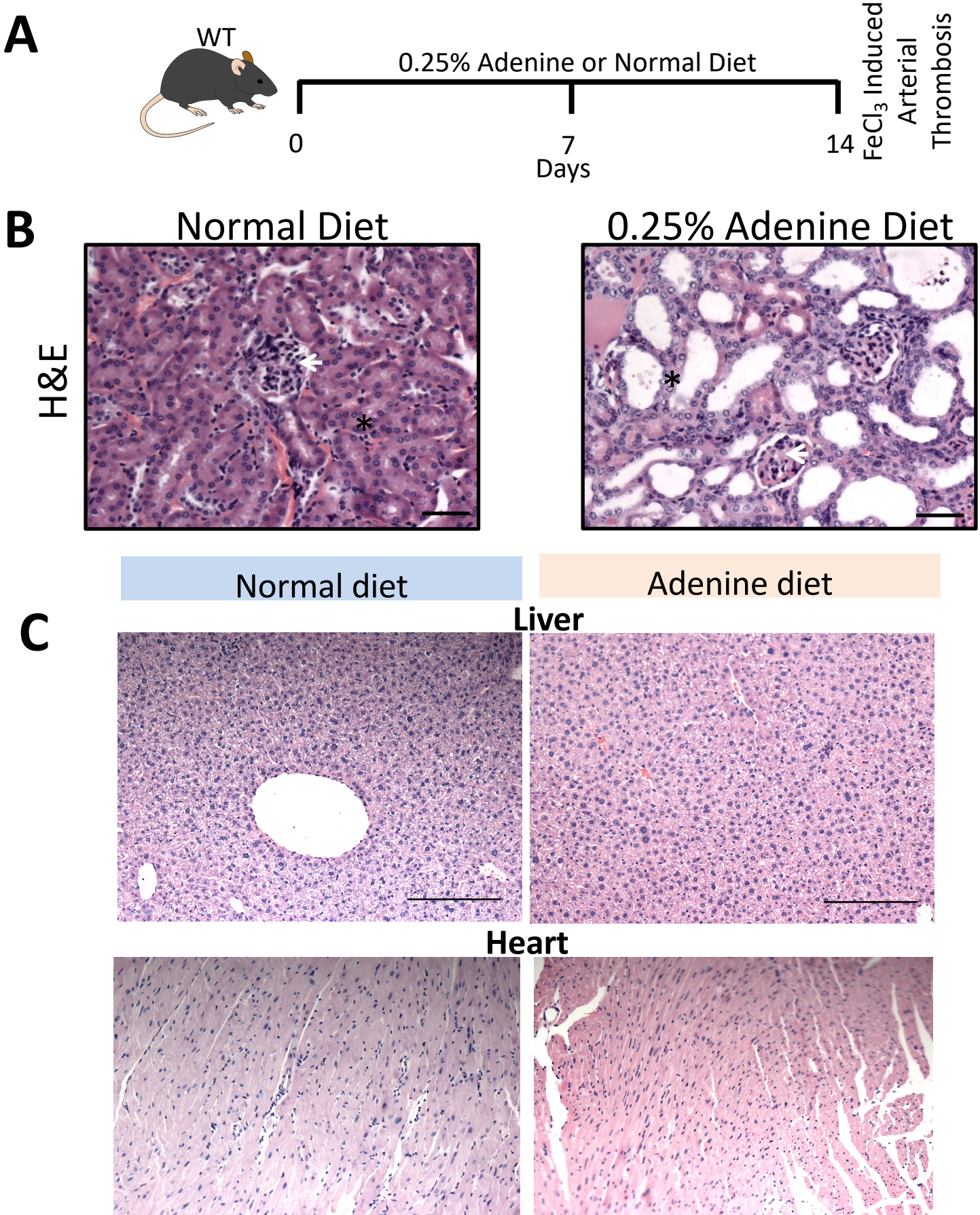

Supplementary Figure 2

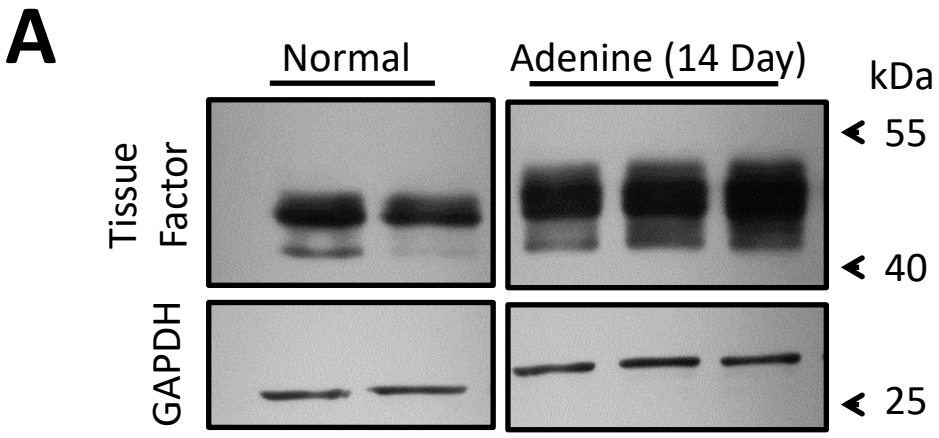

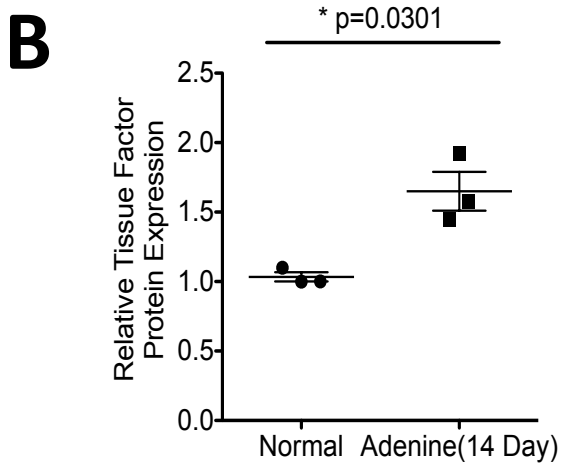

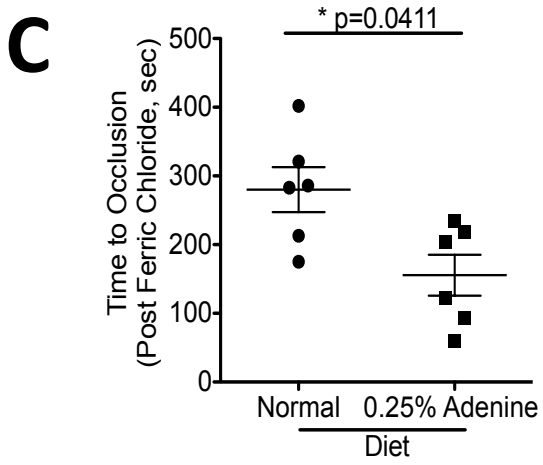

Supplementary Figure 3